LBL-15227

Lawrence Berkeley Laboratory
UNIVERSITY OF CALIFORNIA

EARTH SCIENCES DIVISION

GMINC - A MESH GENERATOR FOR FLOW SIMULATIONS IN FRACTURED RESERVOIRS

K. Pruess

March 1983

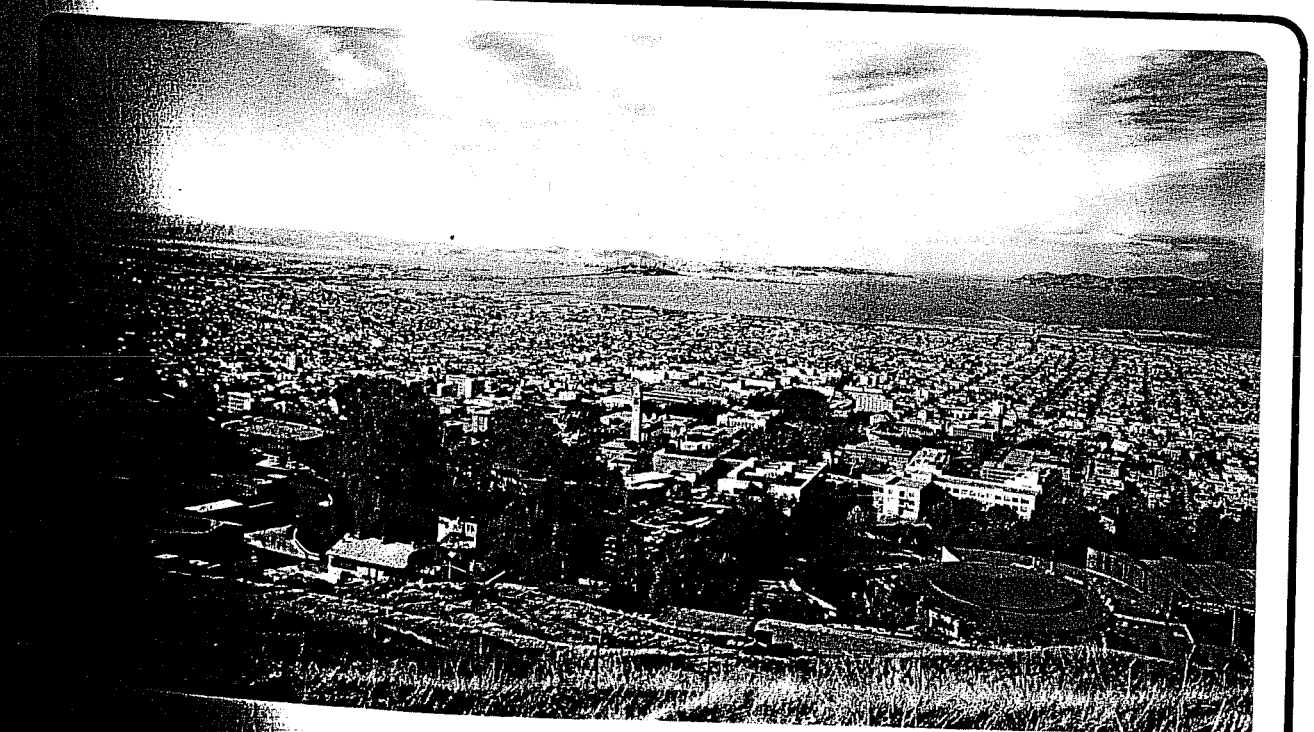

...red for the U.S. Department of Energy under Contract DE-AC03-76SF00098

Printed in the United States of America
Available from
National Technical Information Service
U.S. Department of Commerce
5285 Port Royal Road
Springfield, VA 22161
Price Code: A04

LBL-15227

GMINC - A Mesh Generator for Flow Simulations In Fractured Reservoirs

Karsten Pruess

Earth Sciences Division
Lawrence Berkeley Laboratory
Berkeley, California 94720

March 1983

ork was supported by the Assistant Secretary for Conservation and Renew-
nergy, Office of Renewable Technology, Division of Geothermal Energy and
ower Technologies of the U. S. Department of Energy under Contract Number
76SF00098.

GMINC - A Mesh Generator for Flow Simulations
In Fractured Reservoirs

TABLE OF CONTENTS

LIST OF TABLES

LIST OF FIGURES

GMINC - A Mesh Generator for Flow Simulations In Fractured Reservoirs

1. Introduction

GMINC is a pre-processor computer program for generating geometrical meshes to be used in modeling fluid and heat flow in fractured porous media. It is based on the method of "multiple interacting continua" (MINC) as developed by Pruess and Narasimhan (1982a,b). The meshes generated by GMINC are in integral finite difference form, and are compatible with the simulators SHAFT79 and MULKOM (Pruess and Schroeder, 1980; Pruess, 1983a). Applications with other integral finite difference simulators are possible, and require slight modifications in input/output formats.

This report describes methodology and application of GMINC, including preparation of input decks and sample problems. A rather comprehensive overview of the MINC-method is also provided to make the presentation self-contained as a guide for modeling of flow in naturally fractured media. However, actual flow simulations are not discussed here; illustrative applications to geothermal problems can be found in (Pruess and Narasimhan, 1982 a, b; Pruess, 1983b; Bodvarsson et al., 1983).

2. Overview of the MINC-Method

2.1 Relationship to double-porosity approach

The method of "multiple interacting continua" (MINC) is conceptually similar and is a generalization of, the well-known double-porosity approach (Barenblatt et al., 1960; Warren and Root, 1963). In the double-porosity approach, a fractured reservoir is partitioned into (1) a primary porosity, which consists of small pores in the rock matrix, e.g. intergranular vugs or vesicles, and (2) a secondary porosity consisting of fractures and joints. Each of the two porosities is treate

as a continuum, whose properties can be characterized by means of the cus... porous medium properties, i.e., permeability, porosity, and compressibil... Flow within each continuum is assumed to be porous flow, governed by Darcy's law.

The important feature of the double-porosity approach is the treatment of "interporosity" flow between rock matrix and fractures. The classical double-porosity work employed a quasi-steady approximation, in which separate averages for the thermodynamic state of the pore fluid are considered in the matrix and in the fractures. The rate of interporosity fluid flow within each reservoir subdomain was assumed to be proportional to the difference in average pressures, P_1-P_2, between primary porosity and fractures. The quasi-steady approximation has been used to develop approximate analytical solutions (Warren and Root, 1963), and it has been incorporated in numerical simulators for flow in naturally fractured reservoirs (Kazemi et al., 1976). This approximation has later been improved by using time-dependent analytical solutions for flow from matrix blocks which are subjected to time-dependent changes in boundary conditions (deSwaan, 1976; Duguid and Lee, 1977; Evans, 1981; Lai et al., 1983). A similar methodology has also been used for modeling the migration of chemical pollutants in fissured rock (Bibby, 1981).

The quasi-steady as well as the analytical approximation to interporosity flow are applicable only to fluids with small and constant compressibility. Analytical approximations can give a more accurate description of interporosity flow, but they are available only for regularly shaped matrix blocks (e.g., slabs, cubes, or spheres). The MINC-method overcomes these restrictions by treating interporosity flow entirely by numerical methods. This makes possible a fully transient description of interporosity flow, which is applicable to problems with coupled fluid and heat flow, and to multiphase, multicomponent fluids with large and varying compressibilities, such as steam-water mixtures. Also, the MINC-method

is applicable to flow systems with irregular and stochastic fracture distributions.

Before going further it should be mentioned that several authors have previously presented a numerical treatment of interporosity flow (Kazemi, 1969; Coats, 1977; Gilman and Kazemi, 1982). This has substantiated the approximations made in earlier analytical treatments, while overcoming some of the limitations. However, the numerical work was limited to highly idealized regular distributions of a small number of fractures, or to highly symmetrical fracture patterns. Accurate description of interporosity flow requires a resolution of the pressure- and temperature-gradients at the matrix/fracture interface. In the numerical approaches mentioned above this was achieved by explicit partitioning of the flow domain into "small" simply-connected grid blocks, as in conventional porous medium simulators. This type of approach is unsuitable for naturally fractured reservoirs with ubiquitous fractures, where it would lead to excessively large numbers of grid blocks.

The MINC-method employs a novel concept for partitioning of the rock matrix into computational volume elements, which is suitable for flow systems with fractures too numerous to be accounted for individually and explicitly. The method follows the double-porosity approach in assuming that global flow in the reservoir occurs only through the system of interconnected fractures, which, furthermore, is approximated as a continuum. Long et al. (1982) have shown that networks of finite fractures may exhibit characteristics quite different from those of a porous medium. From a phenomenological viewpoint, however, there is some justification in characterizing a fracture system by means of customary porous medium parameters. This is the approach adopted in the MINC-method. The fracture system and the matrix blocks are each represented as a porous medium-type continuum. To obtain a fine resolution of gradients which drive interporosity flow, the matrix continuum is further partitioned into a series of sub-continua, and the double-porosity approach is extended to a method of multiple inter

acting continua. We shall now proceed to explain the partitioning method in detail.

2.2 The partitioning scheme

The crucial point of the MINC-method is the partitioning (or discretization) procedure adopted for interporosity flow. We shall here present a fundamental principle on which partitioning must be based, and shall then proceed to apply the principle to naturally fractured flow systems.

In order to numerically model flow processes in geothermal reservoirs (or, for that matter, in any subsurface flow systems), it is necessary to partition the system under study into a number of volume elements V_n ($n = 1, 2, \ldots, N$). Then the appropriate conservation equations for mass, energy, and momentum can be written down for each volume element (see Appendix A). These equations hold true irrespective of size, shape, heterogeneities, etc. of the volume elements V_n (Narasimhan, 1982). This geometric flexibility can be most fully exploited within an integral finite difference formulation, which is locally one-dimensional, avoiding any reference to a global coordinate system (Edwards, 1972). However, the conservation equations in integral finite difference form are useful only if the allowable partitions V_n ($n = 1, \ldots, N$) are suitably restricted on the basis of geometric and thermodynamic considerations. Indeed, to obtain practically solvable equations, we need to be able to relate fluid and heat flow between volume elements to the accumulation of fluid and heat within volume elements.

The accumulation terms for mass and heat (left hand sides of Equations A.1, A.2) determine the average values of thermodynamic parameters within volume elements. Fluid and heat flows are driven by gradients of pressure and temperature, respectively, and these can be expressed in terms of average values of thermodynamic variables if and only if there is approximate

of
odynamic equilibrium within each volume element at all times. This leads us
to the following:

Principle of partitioning: For purposes of numerical modeling, a flow domain must be partitioned, or discretized, in such a way that there is approximate thermodynamic equilibrium in all volume elements at all times.

porous media, thermodynamic conditions normally vary continuously and smoothly with position, so that this principle will be satisfied if volume elements are chosen as "sufficiently" small simply-connected regions. The situation can be quite different in fractured media, where changes in thermodynamic conditions as a consequence of boiling or cold water injection may propagate rapidly in the fracture network, while migrating only slowly into the rock matrix. Thus, thermodynamic conditions may vary strongly with position in the vicinity of the fractures. Variations in thermodynamic conditions will be much less pronounced in the direction of a fracture than perpendicular to it. This suggests that changes in thermodynamic conditions in the matrix will locally depend primarily upon the distance from the nearest fracture, with interporosity flow being perpendicular to the fracture faces.

Based on these consideration, the MINC-method makes the approximation to partition the rock matrix into sequences of nested volume elements, which are defined on the basis of distance from the fractures. For the case of an idealized fracture distribution as shown in Figure 1, this concept gives rise to a computational mesh as shown in Figure 2. Modeling of fluid and heat flow for such a system of nested volume elements, or interacting continua, is straightforward within an integral finite difference formulation. The matrix-fracture interaction is described in purely geometrical terms, and the

elevant geometric quantities, i.e., element volumes, interface areas, and
odal distances, can be easily obtained in closed form (Pruess and Narasimh
982a).

The partitioning concept based on distance from the nearest fracture
can be readily extended to arbitrary irregular fracture distributions. Figure
illustrates this for a set of fractures of finite length. Depending upon the
problem at hand, it may first be necessary to eliminate the dead-end portions
of the fractures, which do not participate in global flow within the fracture
system (Figure 3b). The rock matrix can then be readily partitioned into several
continua with increasing distance from the fractures (Figure 3c). While the
general case of irregular fractures is straightforward from the conceptual point
of view, it is not generally possible to obtain the geometrical parameters for
the sub-continua in an explicit analytical fashion. As shown by Pruess and
Karasaki (1982), all geometric parameters for interporosity flow in systems with
irregular fractures can be computed numerically from a scalar function, which
expresses the proximity of matrix material to the fractures, and is therefore
termed a "proximity function". This function can be easily calculated for any
given (regular or irregular) fracture distribution. Before we introduce the
concept of proximity function, it is desirable to further generalize the parti-
tioning scheme outlined above. This can be done by adopting a scaling procedure,
which in effect lumps several disjoint subcontinua together into one computational
volume element.

2.3 Scaling

Referring again to the basic MINC-partitioning as shown in Figure 2, one
can argue that often it may not be necessary to have separate volume elements
within each of the rock matrix blocks depicted in Figure 2. Depending on the

...le of the blocks and on the distance from sinks or sources, thermodynamic ...nditions in corresponding continua in neighboring blocks may be very similar. ...erefore it may be possible to lump corresponding continua from several blocks, ...entified by index numbers in Figure 2, into one computational volume element. ...e geometric parameters pertaining to such a lumped partitioning can be readily ...btained from those for a single matrix block by means of a simple scaling ...peration. For an idealized fracture distribution as shown in Figure 1, a domain ...of volume V_n contains $\sigma = V_n/D^3$ matrix blocks. If corresponding continua ...within the domain V_n are lumped together, each sub-continuum appears σ times, ...so that the total volume of continuum j becomes

$$V_j \rightarrow V'_j = \sigma V_j \tag{1}$$

Here, V_j is the volume of continuum j in one matrix block, and V'_j is the volume of continuum j in the domain V_n.

Similarly, each interface area appears σ times in domain V_n so that

$$A_{j_1, j_2} \rightarrow A'_{j_1, j_2} = \sigma A_{j_1, j_2} \tag{2}$$

where A'_{j_1, j_2} is the total interface area between continua j_1 and j_2 in the domain V_n. Nodal distances, however, are independent of the number of continua lumped together, so that

$$d_{j_1, j_2} \rightarrow d'_{j_1, j_2} = d_{j_1, j_2} \tag{3}$$

From the way in which the scaling laws (1) through (3) were derived, they are applicable and valid when an integral number of matrix blocks are lumped ($\sigma = 1,2,3 \ldots$). It is very convenient, however to generalize by applying the same scaling laws to domains of arbitrary size or shape, including the case where $V_n << D^3$, i.e., $\sigma << 1$. In this way it becomes possible to associate a series of interacting continua to any reservoir subdomain, including the limit $V_n \rightarrow 0$. As will be discussed below, the concept of

scaling is even more important for stochastic than for regular fracture distributions. It makes it possible to refer all geometric parameters for sub-continua to one single representative sub-domain of the reservoir, rather than re-evaluating them for each volume element.

2.4 The mesh construction

In the MINC-method, a computational mesh for a naturally fractured reservoir is obtained in two steps. The first step is to construct a mesh just as would be done for a porous medium-type system, based on considerations of global geometry, symmetry, and desired overall spatial resolution ("primary mesh"). The primary mesh is specified in integral finite difference form by means of a set of volume elements V_n ($n = 1, \ldots, N$), interface areas A_{nm}, and nodal distances d_{nm}. The second step is to sub-partition each grid block V_n of the primary mesh into a sequence of interacting continua V_{nj} ($j = 1, \ldots, J$) based on some specific characterization of the fracture distribution. Global flow ("interblock flow") occurs exclusively in the fracture system, whereas rock matrix and fractures interact locally within the grid blocks of the primary mesh ("intrablock flow"). Therefore, all "connections" (A_{nm}, d_{nm}) of the primary mesh are assigned to the fracture system. Additional "intrablock" connections are generated to permit flow between V_{nj} and V_{nj+1} ($n = 1, \ldots, N$; $j = 1, \ldots, J - 1$). The complete calculational mesh, containing all primary volume elements, the connections for global flow in the fracture system, and all sub-continua and connections for interporosity flow, is referred to as the "secondary" mesh.

Concluding remarks

The MINC-method provides a rather substantial simplification of the complex problem of flow in a naturally fractured rock mass. It is not a patent recipe, but an approximation whose validity should be carefully evaluated before it is applied to specific problems. The concept of partitioning the rock matrix according to distance from the fractures is expected to be very accurate for certain systems and processes, while giving adequate engineering accuracy in others, but being poor or inapplicable in some areas.

At present, there is little quantitative information available regarding the range of applicability of the MINC-method, and the accuracy which can be achieved for different types of flow systems and processes. In this section we present some considerations which should serve as a guide in applications.

The central approximation made in the MINC-method is that thermodynamic conditions in the rock matrix are considered to depend only on the distance from the nearest fracture. This is an approximation which, strictly speaking, will almost never be rigorously valid in actual flow problems. It is helpful, therefore, to discuss conditions under which the "distance only" approximation, though not rigorously valid, will nevertheless accurately predict interporosity flow.

A favorable case for the MINC-method exists when (i) initial thermodynamic conditions in matrix blocks depend approximately only on the distance from the fractures (an important special case is uniform initial conditions in matrix blocks), and when (ii) imposed transient changes in thermodynamic conditions in the fractures occur in such a way that matrix blocks are subjected to approximately uniform boundary conditions at all times. Even under these very restricted conditions, the "distance only" approximation is not strictly valid. It breaks down near fracture intersections, because effects of interporosity flow to or

from several fractures overlap. For the MINC-method to be applicable, however, actually something less than validity of the "distance only" approximation is required. In fact, this approximation needs to be valid only "on the average" in the sense that gradients of pressure and temperature, calculated on the basis of the "distance only" approximation, will yield the proper total rates of fluid and heat flow when fluxes are integrated over an interface area at a given distance from the matrix block faces. Numerical and analytical studies performed by Lai et al. (1983) have shown that for a large class of problems this is indeed the case.

Lai et al. examined the flow of heat or fluid with small and constant compressibility from regularly shaped matrix blocks with uniform initial conditions, which are subjected to a uniform step change in boundary conditions at the surface. The analytical Fourier series solution available for this type of problem yields curved isobaric or isothermal surfaces (Carslaw and Jaeger, 1959). The MINC-method on the other hand approximates these surfaces as planes which are parallel to the block faces, overpredicting thermodynamic parameters in some parts of the surface, while underpredicting them in others. However, when total flow rates across interfaces at a fixed distance from the block faces are computed, by areal integration, these deviations average out to near zero, yielding rates which are accurate to within a fraction of a percent. It is to be expected that the MINC-method should yield similarly accurate predictions for interporosity flow rates in multiphase flow problems with capillarity and relative permeability effects, as long as matrix blocks are subjected to approximately uniform boundary conditions.

Matrix blocks will experience approximately uniform boundary conditions if spatial variations of thermodynamic conditions in the fracture system are insignificant over block dimensions. Generally speaking, therefore, conditions

be favorable for application of the MINC-method if matrix blocks are "small" comparison to characteristic dimensions of the problem at hand. Where this is the case, interporosity flow will be poorly predicted by the MINC-method. MINC-approximation may still be applicable in these cases, however, if only a latively small number of matrix blocks are subjected to non-uniform boundary nditions at any given time, with most interporosity flow involving matrix locks having approximately uniform boundary conditions. This type of situation ay arise in problems with propagating phase fronts (or thermal fronts). If matrix block dimensions are small in comparison to the spatial extent of zones with different phase compositions (or different temperatures), the matrix blocks at the phase (or temperature) front will make a small contribution to interporosity flow, so that the MINC-approximation is valid for all except a few matrix blocks.

Further insight can be gained by examining the forces which govern fluid flow in fractured porous media. These are (i) externally applied pressures, (ii) viscous friction, (iii) capillarity, and (iv) gravity. Of these, the first three are compatible with approximating thermodynamic conditions in the matrix as depending on the distance from the fractures only. Gravity presents special problems, because it will introduce a directional dependence of interporosity flow. Furthermore, it can cause thermodynamic conditions in matrix blocks to depend on the vertical component of distance, and it gives rise to phase segregation in the fractures, with non-uniform boundary conditions for some matrix blocks.

It is easy to show that gravity effects on interporosity flow will vanish for matrix blocks with no internal phase segregation, which are subjected to uniform boundary conditions by the surrounding fractures. The gravity contribution to the interporosity flow for phase β in this case is (see equation A.3):

$$\int_{\Gamma_n} \frac{k_\beta \rho_\beta^2}{\mu_\beta} \underset{\sim}{g} \cdot \underset{\sim}{n}\, d\Gamma = \left(\frac{k_\beta \rho_\beta^2}{\mu_\beta}\right)_{\Gamma_n} \int_{\Gamma_n} \underset{\sim}{g} \cdot \underset{\sim}{n}\, d\Gamma = \left(\frac{k_\beta \rho_\beta^2}{\mu_\beta}\right)_{\Gamma_n} \int_{V_n} \operatorname{div} \underset{\sim}{g}\, dV$$

Here the mobility terms could be pulled in front of the integral, because it has been assumed that thermodynamic conditions in the matrix would depend only on the distance from the surface. This is of course an oversimplification, because in multiphase systems with different phase densities gravity will induce segregation both inside matrix blocks and in the fractures. Favorable conditions for application of the MINC-method will still exist if matrix block thickness is small in comparison to the thickness of layers with different phase composition.

This discussion may be summarized as follows:

- The MINC-approximation is expected to be most accurate for flow systems with ubiquitous fractures and "small" matrix blocks, in which most blocks experience approximately uniform boundary conditions at all times.
- Generally favorable for application of the MINC-method are single-phase flow problems, or problems with low matrix permeability, where interporosity flow is mostly heat conduction. In these cases gravity effects on interporosity flow will be either absent or small.
- Multiphase systems can be handled if matrix block dimensions are small in comparison to dimensions of regions with different phase compositions, or if density differences between the phases are "not too large".
- Transport of chemical species in fractured rock masses should be amenable to a MINC-type representation, as species migration between matrix and fractures should be little affected by gravity. This will hold for chemical pollution in fissured systems, and for

processes of ore formation in veins. Wall rock alterations in hydrothermal mineral systems are known to often depend primarily on the distance from the veins.

- An attractive area of application may be in the chemical processing industry for heterogeneous reactions between a solid granular material, and fluids or gases (Rasmuson and Neretnieks, 1980).
- The MINC-approximation is not applicable for systems with large matrix blocks which are subjected to non-uniform boundary conditions for extended time periods. This situation may arise in certain fractured petroleum reservoirs.
- The MINC-approximation is not valid for processes operating on a very long time scale, for which the matrix acts as an avenue for through-flow rather than one-way flow. An example of this would be a steady-state flow field in the matrix/fracture system.

3. Proximity Functions

3.1 The concept

For any given reservoir subdomain with known fracture distribution, a function V(x) can be defined, which represents total matrix volume V within a distance x from the fracture faces. Note that the volume V will generally consist of a finite number of disjoint multiply-connected regions, representing a quite complex topological structure (see Figure 3c). If V_o is the volume of the subdomain, and ϕ_1 is the volume fraction (average porosity) of the fracture system, the volume of the fracture continuum within V_o is $V_1 = \phi_1 . V_o$. It is convenient to introduce a "proximity function" PROX(x), which expresses, for a given reservoir subdomain V_o, the total fraction of matrix volume within a distance x from the fractures. Noting that the total matrix volume in domain V_o is

$$V_m = (1-\phi_1)\, V_o \tag{5}$$

we have

$$PROX(x) = \frac{V(x)}{V_m} = \frac{V(x)}{(1-\phi_1)\, V_o} \tag{6}$$

3.2 Relationship to discretization

In the MINC-method, a discretization is adopted for the rock matrix (see Figure 4) whereby all matrix volume within a distance x_2 from the fracture faces will be lumped into one computational volume element (or subcontinuum) V_2; matrix volume within a distance larger than x_2 but less than x_3 will be lumped into V_3, etc. This is illustrated in Figure 4 for a regular fracture network, but it is evident that the same procedure can be applied to arbitrary irregular fracture distributions, see Figure 3c. To define flow towards or away from the fractures, it is necessary to specify interface areas and nodal distances between the matrix sub-continua. From the definition of the proximity function as given above, the interface area for flow at distance x is simply

$$A(x) = \frac{dV}{dx} = (1-\phi_1)\, V_o \frac{d\ PROX\ (x)}{dx} \tag{7}$$

In conventional porous medium-type simulation methods with simply-connected grid blocks, the computational nodes are points, usually located at the center of a volume element. For the multiply-connected volume elements of the MINC-method, the element nodes become nodal surfaces, which are located half-way between the inner and the outer surface of an element. (Note that the interfaces between elements will not in general be halfway between neighboring nodal surfaces). A discretization based on distance from the fractures can be uniquely specified by means of a set of volume

tions ϕ_j (j=1, ..., J). Here ϕ_1 is the average fracture porosity, and the ..., ϕ_J denote volume fractions in the matrix at increasing distance from fractures. Obviously we must have

$$\sum_{j=1}^{J} \phi_j = 1 \tag{8}$$

Apart from this constraint, the ϕ_j (j=2, ..., J) are arbitrary, but for best accuracy the volume fractions near the fractures (ϕ_2, ϕ_3, ...) should be chosen not "too" large. The volumes of the sub-partitioning are simply

$$V_{nj} = V_n \cdot \phi_j \tag{9}$$

so that

$$\sum_{j=1}^{J} V_{nj} = V_n \tag{10}$$

In the "secondary" mesh $\{V_{nj}; n=1, ..., N; j=1, ...,J\}$ each of the primary grid blocks V_{n1} (representing fractures) interacts with its neighbors through the fracture continuum, and with a one-dimensional string V_{n2}, V_{n3},..., V_{nJ} of nested grid "blocks " in the matrix (see Figure 5). The distances x_j to which the V_{nj} extend can be simply obtained by inverting the proximity function. We have, for j=2, 3, ..., J

$$PROX(x_j) = \sum_{j'=2}^{j} \frac{\phi_{j'}}{1-\phi_1} \tag{11}$$

The interface area between elements V_{nj} and V_{nj+1} is simply $A(x_j)$ as given by equation (7), with V_o replaced by the volume V_n of the primary element:

$$A_{nj,\, nj+1} = (1-\phi_1)\, V_n \left.\frac{d\ PROX(x)}{dx}\right|_{x_j} \tag{12}$$

It should be noted that Equation (12) implies an application of the "scaling" concepts, as outlined in section 2.3. The proximity function of a flow system is defined once and for all for a certain representative domain V_o, and is normalized to unit matrix volume [cf. Equation (6)]. Therefore, the derivative dPROX/dx gives an interface area per unit matrix volume, which in Equation (12) is properly scaled to the matrix volume present in V_n.

While this procedure is practically convenient, it is recognized that naturally fractured systems may exhibit "scale effects" (Long et al., 1982); i.e., average properties may depend on the scale of observation. The use of one single proximity function for a flow system as implied in Equation (12) ignores scale effects. If it is desired to take such effects into account, one could use a different proximity function $PROX_n(x)$ for each volume element V_n of the primary mesh.

Nodal distances are given by (j=2, ..., J-2)

$$d_{nj,\,nj+1} = \frac{x_{j+1} - x_j}{2} + \frac{x_j - x_{j-1}}{2}$$

$$= \frac{1}{2}\,(x_{j+1} - x_{j-1}) \qquad (13)$$

The fracture nodes are placed at the fracture-matrix interface, so that

$$d_{n1,\,n2} = \frac{x_2}{2} \qquad (14)$$

The innermost nodal distance requires special consideration. Writing

$$d_{nJ-1,\,J} = \frac{x_{J-1} - x_{J-2}}{2} + D_J \qquad (15)$$

we introduce the distance D_J of the nodal surface with index J from the innermost interface area, $A_{nJ-1,\,nJ}$. D_J should be chosen in such a way that the finite difference approximation for pressure - and temperature - gradients

give the most accurate estimate for the actual gradient at interface $A_{nJ-1, nJ}$, so that flow between V_{nJ-1} and V_{nJ} will be described accurately. In a transient problem, D_J will be a function of time. The "best" time-independent estimate for D_J uses the value appropriate for quasi-steady flow. This depends upon the dimensionality of the problem, and on the average linear dimensions of the innermost grid block. The following table holds for rectangular matrix blocks (cf. Warren and Root, 1963):

Table 1. Quasi-steady flow distances for rectangular matrix blocks.

Case	Dimensions of matrix blocks	Dimensions of innermost blocks	Average linear dimension of innermost block	D_J
1-D	a	$u=a-2x_{J-1}$	$\ell = u$	$\ell/6$
2-D	a	$u=a-2x_{J-1}$	$\ell = \frac{2uv}{u+v}$	$\ell/8$
	b	$v=b-2x_{J-1}$		
3-D	a	$u=a-2x_{J-1}$		
	b	$v=b-2x_{J-1}$	$\ell = \frac{3uvw}{uv+vw+uw}$	$\ell/10$
	c	$w=c-2x_{J-1}$		

GMINC uses these values for D_J irrespective of the shape of the matrix blocks. This approximation will be accurate provided the discretization is not too coarse (i.e., ϕ_J should not be much larger than ϕ_{J-1}).

4. General Description of Program GMINC

GMINC carries out the numerical operations necessary to transform a porous medium-type "primary" mesh, into a "secondary" mesh which incorporates global flow in the fracture system, and local "interporosity" flow between fractures and rock matrix.

The input to GMINC consists of:

(a) a "primary" mesh, as would commonly be used to model transport in porous media. The primary mesh is specified in integral finite difference form by means of a set of volume elements V_n (n=1, ..., N), interface areas A_{nm}, and nodal distances d_{nm}.

(b) parameters or functions which characterize fracture distributions. GMINC contains a proximity function routine "PROX(x)", which offers a choice of several different proximity functions and parameters for regularly shaped matrix blocks. Generally speaking, the user will have to write his/her own proximity function subprogram, appropriate for the fracture distribution at hand, and incorporate it into GMINC. Appendix B gives some illustrative examples.

(c) a set of parameters specifying the discretization procedure to be applied for the fractured system. As discussed above, this is done in terms of a set of volume fractions ϕ_j (j=1, ..., J), with J denoting the total number of interacting continua.

GMINC has a very simple main program, which calls three subroutines: PRIMESH, GEOMINC, and MINCME. PRIMESH reads all input data, namely, the parameters of the "primary" mesh, and the parameters for the volume fractions of the sub-partitions. GEOMINC computes all geometric parameters (element volumes, interface areas, nodal distances) for the secondary mesh, normalized to a domain of unit volume. MINCME works sequentially through the volume elements of the primary mesh and, using the scaling procedure outlined in section 2.3, scales the parameters generated by GEOMINC to generate the secondary mesh. Routine GEOMINC uses the proximity function subprogram PROX(x), and a subroutine INVER, to solve equations (11) and (12) for nodal distances and interface areas, respectively. Inversion of PROX(x) is

carried out by means of a sequence of bisecting nested intervals (subroutine INVER).

Three disk files are used by the program. TAPE4 holds a list of primary volume elements, TAPE14 holds the output of volume elements as obtained from the MINC partitioning process, and TAPE15 holds all interface areas and nodal distances of the secondary mesh. TAPE14 and TAPE15 are compatible with SHAFT79 or MULKOM input formats; merged together they make up the "MESH" file required by these simulators.

Volume elements are referred to by five character "names", with the following convention. The first two characters are arbitrary (alphanumeric). Character #3 is alphanumeric on input, and on output is changed into "1" (for fracture elements) or "A" through "Z" (for matrix elements). Here "A" signifies the matrix element which is closest to the fractures, "B" is the second closest element, etc. The last two characters of an element name are numbers. Examples will be given in Section 6.

5. Preparation of Input Decks for GMINC

The input of GMINC is organized in "blocks", as indicated in the following table.

Table 2. Input Data Blocks

Block	Description
ELEME	List of elements of primary mesh.
CONNE	List of interfaces (connections) of primary mesh.
PART	Parameters for defining the partitioning procedure.
ENDMI (Last card)	One card closing the GMINC input deck.

The data blocks "ELEME", "CONNE", and "PART" can be provided in arbitrary order. A sequence of identical elements or connections can be specified on a single data card. Figure 6 summarizes the input data; the detailed description of input is as follows.

ELEME	introduces element information.
Card ELEME.1	Format (A3, I2, 2I5, A3, A2, E10.4) EL, NE, NSEQ, NADD, MA1 MA2, VOLX
EL, NE	5-character code name of an element. The first three characters are arbitrary, the last two characters must be numbers.

NSEQ — number of additional elements having the same volume and belonging to the same reservoir domain.

NADD — increment between the code numbers of two successive elements. (Note: the maximum permissible code number NE + NSEQ * NADD is 99.)

MA1, MA2 — a five character identifier specifying the reservoir domain to which the element belongs. The first character must not be an "M". On output, the fractured medium is assigned the same domain identifier as was input. For rock matrix elements, the first character of the material identifier is changed into "M".

VOLX — element volume (m^3).

Repeat card ELEME.1 for any number of elements desired.

Card ELEME.2 — A blank card closes the ELEME data block.

CONNE — introduces information for the connections (interfaces) between elements.

Card CONNE.1 — Format (A2, A1, I2, A2, A1, I2, 4I5, 4E10.4)
EL1, E1, NE1, EL2, E2, NE2, NSEQ, NAD1, NAD2, ISOT, D1, D2, AREAX, BETAX

EL1, E1, NE1 — code name of the first element.

EL2, E2, NE2 — code name of the second element.

NSEQ — number of additional connections in the sequence.

NAD1 — increment of the code number of the first element between two successive connections.

NAD2 — increment of the code number of the second element between two successive connections.

ISOT — set equal to 1, 2, or 3; specifies absolute permeabili... to be PER(ISOT) for the materials in elements (EL1, E1, N... and (EL2, E2, NE2), where PER is read in block ROCKS in... SHAFT79 or MULKOM. This allows assignment of different... permeabilities, e.g., in the horizontal and vertical dir...

D1
D2 — Distance (m) from center of first and second element, respe... tively, to their common interface.

AREAX — interface area (m^2)

BETAX — cosine of the angle between the gravitational acceleration vector and the line between the two elements.

Repeat card CONNE.1 for any number of connections desired.

Card CONNE.2 a blank card closes the CONNE data block.

Note: If no interblock connections are desired, it is still necessary to input the data block "CONNE". In this case the card "CONNE" would be followed immediately by a blank card.

PART TYPE introduces information on the partitioning procedure, and selects the type of proximity function to be used.

Format (2A5)

PARTb, TYPE

PART — identifier of data block with partitioning parameters.

TYPE — a five-character word for selecting one of the six different proximity functions provided in GMINC.

ONE-D: a set of plane parallel infinite fractures with matrix block thickness between neighboring fractures equal to PAR(1).

TWO-D: two sets of plane parallel infinite fractures, with arbitrary angle between them. Matrix block thickness is PAR (1) for the first set, and PAR (2) for the second set. If PAR (2) is not specified explicity, it will be set equal to PAR(1).

THRED: three sets of plane parallel infinite fractures at right angles, with matrix block dimensions of PAR(1), PAR(2), and PAR(3), respectively. If PAR(2) and/or PAR(3) are not explicity specified, they will be set equal to PAR(1) and/or PAR(2), respectively.

STANA: average proximity function for rock loading of Stanford large reservoir model (see appendix B).

STANB: proximity function for the five bottom layers of Stanford large reservoir model.

STANT: proximity function for top layer of Stanford large reservoir model.

Note: a user wishing to employ a different proximity function than provided in GMINC needs to replace the function subprogram PROX(x) with a routine of the form:

```
FUNCTION PROX(x)

PROX = (arithmetic expression in x)

RETURN

END
```

It is necessary that PROX(x) is defined even when x exceeds the maximum ible distance from the fractures, and that PROX = 1 in this case. Also, the user supplies his/her own proximity function subprogram, the parameter has to be chosen equal to ONE-D, TWO-D, or THRED, depending on the dimen- ality of the proximity function. This will assure proper definition of most nodal distance (see section 3.2).

Card PART.1 Format (2I3, A4, 7E10.4)

J, NVOL, WHERE, (PAR(I), I=1,7)

J total number of multiple interacting continua ($J \leq 25$).

NVOL total number of explicitly provided volume fractions ($NVOL \leq J$, see section 3.2). If $NVOL < J$, the volume fractions with indices NVOL+1, ..., J will be internally generated; all being equal and chosen such as to satisfy Equation (8).

WHERE specifies whether the sequentially specified volume fractions begin with the fractures (WHERE=OUTb) or in the interior of the matrix blocks (WHERE = INbb).

PAR(I), I=1,7 holds parameters for fracture spacing (see above).

Card PART.2.1, 2.2, etc.

Format (8E10.4)

(VOL(I), I = 1,NVOL)

VOL(I) volume fraction (between 0 and 1) of continuum with index I (for WHERE = OUTb) or index J+1-I (for WHERE = INbb). NVOL volume fractions will be read. For WHERE = OUTb, I = 1 is the fracture continuum, I = 2 is the matrix continuum closest to the fractures, I = 3 is the matrix continuum adjacent to I-2, etc.

ENDMI closes the GMINC input deck.

Sample Calculations

The problems presented in this section are intended to illustrate applications of GMINC. It was pointed out before that the partitioning scheme for a fractured reservoir mesh works sequentially through the volume elements of the primary mesh on a grid-block-by-grid-block basis. The calculational procedure is the same irrespective of whether the primary mesh has a few or many grid blocks, and irrespective of the dimensionality of the primary mesh. Therefore, it is sufficient to consider small primary meshes in the following examples.

(a) One-block problem

The GMINC input deck for this example is given in Figure 7 (the file "GMINCG" used here is a compiled version of GMINC). The primary mesh consists of just one grid block, with no primary (interblock) connections present. It is partitioned into 10 continua, with volume fractions increasing away from the block faces. The type of proximity function chosen ("THRED") corresponds to three orthogonal fracture sets. Matrix block dimensions are PAR(1) = PAR(2) = PAR(3) = 50 m, with PAR(2) and PAR(3) assigned default values, as these entries are left blank on the data card. Figure 8 shows the table of geometry data as generated by GMINC, scaled for a domain of unit volume. The interface data are always printed between the two volume elements to which they correspond. The complete secondary mesh file is shown in Figure 9. It was obtained by merging the files TAPE14 (holding elements) and TAPE15 (holding connections). On the element header card there appears same information on the partitioning. The mesh file is compatible with SHAFT79 or MULKOM input formats.

(b) Vertical Column

The primary mesh in this example consists of a vertical column of five grid blocks with 100 m thickness and 1 km^2 cross sectional area (see Figure 10). There are two fracture sets, with fracture faces separated by 20 and 40 m distance, respectively. Sub-partitioning is made into 6 continua, with volume fractions for continua #5 and 6 assigned by default. Figure 11 shows the geometry data as generated by GMINC, and Figure 12 gives the complete mesh file for this case.

(c) Radial flow

Figure 13 shows an input deck for a one-dimensional radial mesh of H = 100 m thickness. The first grid block has a radius R_1 = 1 m, and subsequent radial spacings are incremented according to $\Delta R_{n+1} = \alpha \cdot \Delta R_n$, with α = 2.2326074, so that $R_8 = R_1 (\alpha^8-1)/(\alpha-1)$ = 500 m. Sub-partitioning is made into 5 continua, assuming one set of plane parallel fractures with matrix block thickness of 10 m between fracture faces. The geometry data computed by GMINC are shown in Figure 14, and Figure 15 gives the complete secondary mesh file. Note that, because of the one-dimensional fracture geometry, all interface areas within a given volume are equal. A schematic graphic representation of the secondary mesh is shown in Figure 5.

Acknowledgement

The author gratefully acknowledges fruitful discusssions with Dr. T. N. Narasimhan. The help of K. Karasaki with the stochastic fracture calculations is appreciated. Thanks are due to G. S. Bodvarsson and C. H. Lai for a critical reading of the manuscript.

This work was supported by the Assistant Secretary for Conservation and Renewable Energy, Office of Renewable Energy, Division of Geothermal Energy and Hydropower Technologies of the U. S. Department of Energy under Contract No. DE-AC03-76SF00098.

Nomenclature

- a dimension of matrix block (m)
- A interface area (m^2)
- b dimension of matrix block (m)
- c dimension of matrix block (m)
- C specific heat (J/kg°C)
- d nodal distance (m)
- D fracture spacing (m)
- D_J nodal distance for continuum J (m)
- $\underset{\sim}{F}$ mass flux ($kg/m^2 \cdot s$)
- $\underset{\sim}{g}$ gravitational acceleration vector (9.81 m/s^2)
- $\underset{\sim}{G}$ heat flux (W/m^2)
- h specific enthalpy (J/kg)
- J number of interacting continua
- k absolute permeability (m^2)
- K heat conductivity (W/m°C)
- k_β relative permeability for phase β, dimensionless
- $\underset{\sim}{n}$ unit normal vector
- N number of volume elements; also number of Monte Carlo points
- P pressure (Pa)
- q volumetric rate of mass generation ($kg/m^3 \cdot s$)
- Q volumetric rate of heat generation ($J/m^3 \cdot s$)
- R radial distance (m)
- T temperature (°C)
- u specific internal energy (J/kg)
- U volumetric internal energy (J/m^3)

Nomenclature (continued)

V volume (m^3)

V_o reference domain (m^3)

x distance from matrix block face (m)

δ fracture aperture (m)

ϕ volume fraction

Γ surface area (m^2)

ρ density (kg/m^3)

σ number of matrix blocks in domain V_n

μ_β viscosity of phase β (Pa · s)

Subscripts

cap capillary

f fracture

j index number of interacting continuum

ℓ liquid

m matrix; also index number of volume element

n index number of volume element

R rock

v vapor

β phase (β = liquid, vapor)

References

Barenblatt, G. E., I. P Zheltov and I. N. Kochina, 1960. Basic Concepts in the Theory of Homogeneous Liquids in Fissured Rocks, J. Appl. Math. (USSR), Vol. 24 No. 5, pp 1286-1303.

Bibby, R., 1981. Mass Transport of Solutes in Dual-Porosity Media, Water Resources Research, Vol. 17, No. 4, pp. 1075-1081.

Bodvarsson, G. S., Pruess, K., and O'Sullivan, M. J., 1983. Injection and Energy Recovery in Fractured Geothermal Reservoirs, paper SPE-11689, presented at the California Regional Meeting of the SPE, Ventura, California, March.

Carslaw, H. S., and Jaeger, J. C., 1959. Conduction of Heat in Solids, Oxford University Press, Oxford, England, Second Edition.

Coats, K. H., 1977. Geothermal Reservoir Modelling, paper SPE-6892, presented at the 52nd Annual Fall Technical Conference and Exhibition of the SPE, Denver, Col., October.

deSwaan, A. O., 1976. Analytic Solutions for Determining Naturally Fractured Reservoir Properties by Well Testing, Society of Petroleum Engineers Journal, Vol. 16, No. 3, p. 117.

Duguid, J. O., and Lee, P. C. Y., 1977. Flow in Fractured Porous Media, Water Resources Res. Vol. 13 No.3, pp. 558-566.

Edwards, A. L., 1972. TRUMP: A Computer Program for Transient and Steady State Temperature Distributions in Multidimensional Systems, National Technical Information Service, National Bureau of Standards, Springfield, VA.

Evans, R. D., 1981. A Proposed Model for Multiphase Flow Through Naturally Fractured Reservoirs, Paper No. SPE-9940, Society of Petroleum Engineers of AIME, California Regional Meeting, Bakersfield, CA.

Gilman, J. R. and Kazemi, H., 1982. Improvements in Simulation of Naturally Fractured Reservoirs, paper SPE-10511, presented at Sixth SPE-Symposium on Reservoir Simulation, New Orleans, LA.

Hunsbedt, A., Lam, S. T., Kruger, P., and Pruess, K., 1982. Heat Extraction Modeling of the Stanford Hydrothermal Reservoir Model, paper presented at the Eighth Workshop on Geothermal Reservoir Engineering, Stanford University, Stanford, Cal., December.

Iregui, R., Hunsbedt, A., Kruger, P. and London, A. L., 1978. Analysis of Heat Transfer and Energy Recovery in Fractured Geothermal Reservoirs, Stanford Geothermal Program Report SGP-TR-31, Stanford University, Stanford, Ca., June.

Kazemi, H., 1969. Pressure Transient Analysis of Naturally Fractured Reservoirs with Uniform Fracture Distribution, Society of Petrolum Engineers Journal, p. 451-462.

Kazemi, H., Merrill, L. S., Jr., Porterfield, K. L., and Zeman, P. R., 1976. Numerical Simulation of Water-Oil Flow in Naturally Fractured Reservoirs, Society of Petroleum Engineers Journal, pp. 317-326, December.

Lai, H.S., G.S. Bodvarsson, and K. Pruess, 1983. Verification of the MINC-Method in preparation.

Lai, C. H., Bodvarsson, G. S., Tsang, C. F., and Witherspoon, P. A., 1983. A New Model for Well Test Data Analysis for Naturally Fractured Reservoirs, paper SPE-11688, presented at the 1983 California Regional Meeting of the SPE, Ventura, Ca.

Long, J. C. S., Remer, J. S., Wilson, C. R., and Witherspoon, P. A., 1982. Porous Media Equivalents for Networks of Discontinuous Fractures, Water Resources Research, Vol. 18, no. 3, 645-658.

Narasimhan, T.N., 1982. Multidimensional Numerical Simulation of Fluid Flow in Fractured Porous Media, Water Resources Research, Vol. 18, No. 4, pp. 1235-1247. August.

Pruess, K., 1983a. Development of the General Purpose Simulator MULKOM, Annual Report 1982, Earth Sciences Division, Lawrence Berkeley Laboratory, to be published.

Pruess, K., 1983b. Heat Transfer in Fractured Geothermal Reservoirs with Boiling, Water Resources Research, Vol. 19, No. 1, pp. 201-208, February.

Pruess, K. and Karasaki, K., 1982. Proximity Functions for Modeling Fluid and Heat Flow in Reservoirs with Stochastic Fracture Distributions, presented at the Eighth Workshop on Geothermal Reservoir Engineering, Stanford University, Stanford, Ca., December.

Pruess, K. and Narasimhan, T. N., 1982a. A Practical Method for Modeling Fluid and Heat Flow in Fractured Porous Media, paper SPE-10509, Proc. Sixth SPE-Symposium on Reservoir Simulation, New Orleans, LA.

Pruess, K., and Narasimhan, T. N., 1982b. On Fluid Reserves and the Production of Superheated Steam from Fractured, Vapor-Dominated Geothermal Reservoirs, Journal of Geophysical Research, Vol. 87, No. B11, pp. 9329-9339.

Pruess, K. and Schroeder, R. C., 1980. SHAFT79 User's Manual, LBL-10861, Lawrence Berkeley Laboratory, Berkeley, Ca., March.

Rasmuson, A. and Neretnieks, I., 1980. Exact Solution of a Model for Diffusion in Particles and Longitudinal Dispersion in Packed Beds, AIChE Journal, Vol. 26, No. 4, pp. 686-690, July.

Warren, J.E. and Root, P.J., 1963. The Behavior of Naturally Fractured Reservoirs, Society of Petroleum Engineers Journal, pp. 245-255.

Witherspoon, P. A., Wang, J. S. Y., Iwai, K., and Gale, J. E., 1980. Validity of Cubic Law for Fluid Flow in a Deformable Rock Fracture, Water Resources Research, Vol. 16, No. 6, pp. 1016-1024.

ppendix A: Mass - and energy - balances

he simulators SHAFT79 and MULKOM solve discretized versions of he following mass-and energy-balance equations:

$$\frac{d}{dt}\int_{V_n}\phi\rho dv = \int_{\Gamma_n}\underset{\sim}{F}\cdot\underset{\sim}{n}d\Gamma + \int_{V_n} q dv \qquad (A.1)$$

$$\frac{d}{dt}\int_{V_n} U dv = \int_{\Gamma_n}\underset{\sim}{G}\cdot\underset{\sim}{n}d\Gamma + \int_{V_n} Q dv \qquad (A.2)$$

ass flux is approximated by Darcy's law, which expresses a momentum balance ith negligible inertial force

$$\underset{\sim}{F} = \sum_{\substack{\beta=\text{liquid,}\\ \text{vapor}}} \underset{\sim}{F}_\beta = -k\sum_\beta \frac{k_\beta}{\mu_\beta}\rho_\beta(\nabla P_\beta - \rho_\beta \underset{\sim}{g}) \qquad (A.3)$$

ere we have written mass flux as a sum over liquid and vapor contributions, as is ppropriate for the geothermal case. However, MULKOM can handle flow problems with ny number of phases and components, incorporating suitable generalizations of the quations presented here.

Energy flux contains conductive and convective terms

$$G = -K\nabla T + \sum_\beta h_\beta \underset{\sim}{F}_\beta \qquad (A.4)$$

nd the volumetric internal energy of the rock/fluid mixture is

$$U = \phi\rho u + (1-\phi)\rho_R C_R T \qquad (A.5)$$

The main assumptions made in the above formulation are as follows: (1) the reservoir system is approximated as a mixture of rock and single-component fluid in liquid and vapor form. (2) Liquid, vapor and rock are in local thermodynamic equilibrium, i.e., at the same temperature and (bulk) pressure, at all times. (The effective pressure in phase β is the sum of bulk phase and capillary pressure, $P_\beta = P + P_{cap,\beta}$.)

It is to be noted that the equations given above hold for porous and fractured media alike. Experimental work has established that fracture flow obeys Darcy's law, with fracture permeability related to fracture aperture as (Witherspoon et al., 1980),

$$k_f = \delta^2/12 \qquad (A.6)$$

Appendix B. Examples of proximity functions

(a) One fracture set

The simplest case is a one-dimensional set of plane, parallel, equidistant, infinite fractures with aperture δ and spacing D. The thickness of matrix blocks between neighboring fractures is: $a = D-\delta$ (=PAR(1) on input, card PART.1). To obtain the proximity function, we consider a symmetry element of unit thickness, centered about one fracture. The total matrix volume in this domain is, per unit fracture length, $V_m = a$. The matrix volume within a distance x from the fracture faces is $V(x) = 2x$, so that

$$\text{PROX}(x) = \begin{cases} \dfrac{V(x)}{V_m} = \dfrac{2x}{a} & \text{for } x \leq a/2 \\ 1 & \text{for } x \geq a/2 \end{cases} \qquad \text{(B.1)}$$

(b) Two fracture sets

For two perpendicular sets of plane, parallel, equidistant, infinite fractures the matrix blocks have a rectangular cross section with lengths a and b (corresponding to input parameters PAR(1) and PAR(2), respectively, on card PART.1) The matrix volume per block, per unit of thickness, is $V_m = a \cdot b$. Within a distance x from the fracture faces, the matrix volume is $V(x) = a \cdot b - (a-2x) \cdot (b-2x) = 2(a+b)x - 4x^2$.

Therefore, the proximity function is

$$\text{PROX}(x) = \begin{cases} 2\,\dfrac{a+b}{a \cdot b}\,x - 4\,\dfrac{x^2}{a \cdot b} & \text{for } 2x \leq \min(a,b) \\ 1 & \text{for } 2x \geq \min(a.b) \end{cases} \qquad \text{(B.2)}$$

The same formula holds when the two fracture sets intersect at an arbitrary angle. In that case, a and b are the matrix block dimensions perpendicular to the fracture sets.

(c) Three fracture sets

For three perpendicular sets of plane, parallel, equidistant, infinite fractures, the matrix blocks are parallelepipeds with dimensions a, b, and c (corresponding to input parameters PAR(1), PAR(2), and PAR(3), respectively, on card PART.1). The matrix volume within a distance x from the fractures is, per block, $V(x) = abc - (a-2x)\cdot(b-2x)\cdot(c-2x)$. Defining $u=2x/a$, $v=2x/b$, and $w=2x/c$, the proximity function can be written

$$\text{PROX}(x) = \begin{cases} uvw-(uv+uw+vw)+(u+v+w) & \text{for } 2x \leq \min(a,b,c) \\ 1 & \text{for } 2x \geq \min(a,b,c) \end{cases} \qquad \text{(B.3)}$$

(d) Stanford large reservoir model

For a number of years a laboratory model of a geothermal reservoir has been used at Stanford university for heat extraction experiments (Iregui et al., 1978). The system consists of a large pressure vessel which presently holds a loading of regularly shaped granite blocks (Hunsbedt et al., 1982). There are six layers, each of which has five rectangular blocks and four blc whose cross sections are isosceles rectangular triangles. For the rectangul blocks, the proximity function is given by (B.3). For the triangular blocks straightforward calulation gives

$$\text{PROX}_t(x) = \begin{cases} (3+2\sqrt{2})\,\dfrac{4x^3}{ab^2} - \left[\dfrac{6+4\sqrt{2}}{b^2} + \dfrac{4(2+\sqrt{2})}{ab}\right]x^2 + \left(\dfrac{4+2\sqrt{2}}{b} + \dfrac{2}{a}\right)x & \text{for } x \leq \dfrac{b}{2+\sqrt{2}} \\ 1 & \text{for } x \geq \dfrac{b}{2+\sqrt{2}} \end{cases} \qquad \text{(B.}$$

Here a is the height of the triangular blocks, and $b^2/2$ is their cross secti area.

For heat transfer modeling it is convenient to consider averaged proximity functions in each layer. Denoting the proximity function for the rectangular blocks by $PROX_r(x)$, the average is

$$PROX_{rt}(x) = \frac{5}{7} PROX_r(x) + \frac{2}{7} PROX_t(x) \qquad (B.5)$$

These functions are plotted in Figure 16.

(e) Stochastic fracture distributions

In the general case of arbitrary irregular fracture distributions, proximity functions can be computed by means of Monte Carlo techniques. The method as developed by Pruess and Karasaki (1982) can be summarized as follows. First it is necessary to obtain a specific realization of the stochastic distribution for a domain V_o, and to eliminate isolated and dead-end portions of fractures. This is accomplished with the methods developed by Long et al. (1982). Then a large number N of random points is generated in V_o. For each point, the minimum distance from the fractures is calculated, and all N points are sorted in order of increasing distance. The value of the proximity function for a certain distance x is proportional to the number of points, N(x), with a distance less or equal to x from the fractures. Specifically,

$$PROX(x) = \frac{N(x)}{N} \qquad (B.6)$$

The Monte Carlo procedure provides a discontinuous definition of the proximity function. Before this can be input to GMINC it must be smoothed, e.g. by fitting with a succession of cubic splines. Figure 17 shows an example of a two-dimensional stochastic fracture distribution. The smoothed proximity function obtained with 100,000 random points is shown in Figure 18.

APPENDIX C

GMINC Program Listing

```
      PROGRAM GMINC(INPUT,OUTPUT,TAPE4,TAPE14,TAPE15)

**** GMINC WAS DEVELOPED BY KARSTEN PRUESS
                        AT LAWRENCE BERKELEY LABORATORY. ***********

     THE PROGRAM GENERATES ONE-, TWO-, OR THREE-DIMENSIONAL MESHES
     FOR FLOW SIMULATIONS IN FRACTURED POROUS MEDIA.

     GMINC IMPLEMENTS THE METHOD OF
                    MULTIPLE INTERACTING CONTINUA (MINC)
     AS DEVELOPED BY PRUESS AND NARASIMHAN.

     REFERENCES@

     (1) K. PRUESS AND T.N. NARASIMHAN, A PRACTICAL METHOD FOR
         MODELING FLUID AND HEAT FLOW IN FRACTURED POROUS MEDIA,
         PAPER SPE-10509, PRESENTED AT THE SIXTH SPE-SYMPOSIUM ON
         RESERVOIR SIMULATION, NEW ORLEANS, LA. (FEBRUARY 1982).

     (2) K. PRUESS AND T.N. NARASIMHAN, ON FLUID RESERVES AND THE
         PRODUCTION OF SUPERHEATED STEAM FROM FRACTURED, VAPOR-
         DOMINATED GEOTHERMAL RESERVOIRS, J. GEOPHYS. RES. 87 (B11),
         9329-9339, 1982.

     (3) K. PRUESS AND K. KARASAKI, PROXIMITY FUNCTIONS FOR MODELING
         FLUID AND HEAT FLOW IN RESERVOIRS WITH STOCHASTIC FRACTURE
         DISTRIBUTIONS, PAPER PRESENTED AT EIGTH STANFORD WORKSHOP
         ON GEOTHERMAL RESERVOIR ENGINEERING, STANFORD, CA.
         (DECEMBER 1982).

     (4) K. PRUESS, GMINC - A MESH GENERATOR FOR FLOW SIMULATIONS IN
         FRACTURED RESERVOIRS, LAWRENCE BERKELEY LABORATORY REPORT
         LBL-15227, 1983.

*************************************************************************


-----READ INPUT DATA AND PREPROCESS MESH FILE FOR SEQUENTIAL ELEMENTS--

      CALL PRIMESH

C-----GENERATE INTRABLOCK GEOMETRICAL QUANTITIES FOR A DOMAIN
                                                  OF UNIT VOLUME -----

      CALL GEOMINC

C-----GENERATE COMPLETE MESH FILE ----------------------------------------

      CALL MINCME

      STOP
      END
```

```
      SUBROUTINE PRIMESH
C
      COMMON/MINCDAT/J,NVOL,WHERE,VOL(25),A(25),D(25)
      COMMON/PROXI/L,TYPE(10),PAR(7)
      COMMON/CON/ABC(26)
      DIMENSION VER(4),WORD(5,16)
      DATA VER /5HELEME,5HCONNE,5HPART ,5HENDMI/
      DATA TYPE/5HONE-D,5HTWO-D,5HTHRED,5HSTANA,5HSTANB,5HSTANT/
      DATA ABC/1HA,1HB,1HC,1HD,1HE,1HF,1HG,1HH,1HI,1HJ,1HK,1HL,1HM,1HN,
     X1HO,1HP,1HQ,1HR,1HS,1HT,1HU,1HV,1HW,1HX,1HY,1HZ/
C
      IK=0
 5019 IK=IK+1
      READ 5020,(WORD(IK,I),I=1,16)
 5020 FORMAT(16A5)
C
      DO900 K=1,4
  900 IF(WORD(IK,1).EQ.VER(K)) GOTO920
      PRINT 901,WORD(IK,1)
  901 FORMAT(# HAVE READ UNKNOWN BLOCK LABEL "#,A5,#"  ---  ASSUME ALL#
     X# NEEDED DATA HAVE BEEN READ AND RETURN TO MAIN PROGRAM#)
      RETURN
C
  920 GOTO(1100,1200,1300,1400),K
C
C*****READ ELEMENT DATA.*************************************************
C
 1100 WRITE(4,1101) (WORD(IK,I),I=1,16)
 1101 FORMAT(16A5)
 1102 READ 10,EL,NE,NSEQ,NADD,MA1,MA2,VOLX
   10 FORMAT(A3,I2,2I5,A3,A2,E10.4)
      IF(EL.EQ.3H   .AND.NE.EQ.0) GOTO40
C
      NSEQ1=NSEQ+1
C
C-----GENERATE FILE OF ELEMENT DATA.
C
      DO113 I=1,NSEQ1
      N=NE+(I-1)*NADD
  113 WRITE(4,114) EL,N,MA1,MA2,VOLX
  114 FORMAT(A3,I2,10XA3,A2,E10.4)
      GOTO1102
C
C-----END OF ELEMENT DATA.-------------------------------------------------
C
   40 WRITE(4,41)
   41 FORMAT(#      #)
      GOTO5019
C
C*****READ CONNECTION DATA.**********************************************
C
 1200 WRITE(15,1201)
 1201 FORMAT(#CONNE#)
      NOCONT=0
```

```
1202 READ 20,EL1,E1,NE1,EL2,E2,NE2,NSEQ,NAD1,NAD2,ISOT,D1,D2,AREAX
     X,BETAX
  20 FORMAT(A2,A1,I2,A2,A1,I2,4I5,4E10.4)
     IF(EL1.EQ.2H  .AND.E1.EQ.1H .AND.NE1.EQ.0) GOTO5019
     IF(EL1.EQ.2H++) GOTO5019

     NSEQ1=NSEQ+1

-----GENERATE FILE OF CONNECTION DATA.

     DO23 I=1,NSEQ1
     NOCONT=NOCONT+1
     N1=NE1+(I-1)*NAD1
     N2=NE2+(I-1)*NAD2
  23 WRITE(15,24) EL1,N1,EL2,N2,ISOT,D1,D2,AREAX,BETAX
  24 FORMAT(A2,1H1,I2,A2,1H1,I2,15XI5,4E10.4)
     GOTO1202

-----END OF CONNECTION DATA.----------------------------------------------

****READ DATA FOR MULTIPLE INTERACTING CONTINUA.**********************

***** *J* IS THE NUMBER OF MULTIPLE INTERACTING CONTINUA.
*
***** *NVOL* (.LE.J) IS THE NUMBER OF EXPLICITLY SPECIFIED VOLUME
*      FRACTIONS.
*
***** *WHERE* SPECIFIES WHETHER EXPLICITLY PROVIDED VOLUME FRACTIONS
      ARE GIVEN STARTING AT THE OUTSIDE (FRACTURE) OR INSIDE (MATRIX).
*
***** *PAR* IS AN ARRAY WITH PARAMETERS FOR SPECIFYING FRACTURE
*      DISTRIBUTIONS.

1300 CONTINUE
     DO902 L=1,10
     IF(WORD(IK,2).EQ.TYPE(L)) GOTO 903
 902 CONTINUE
     PRINT 904,WORD(IK,2)
 904 FORMAT(# HAVE READ UNKNOWN PROXIMITY FUNCTION IDENTIFIER  **#A5,**
    X---   STOP EXECUTION#)
     STOP

 903 CONTINUE
-----INDEX *L* LABELS THE TYPE OF PROXIMITY FUNCTION SELECTED.


     READ 1,J,NVOL,WHERE,(PAR(I),I=1,7)
   1 FORMAT(2I3,A4,7E10.4)

-----READ A SET OF VOLUME FRACTIONS-----
     IF(WHERE.EQ.4HOUT ) READ 2,(VOL(M),M=1,NVOL)
     IF(WHERE.EQ.4HIN  ) READ 2,(VOL(J+1-M),M=1,NVOL)
   2 FORMAT(8E10.4)
```

```
C----- END OF MINC-DATA ----------------------------------------------
C
      IF((L.EQ.2 .OR. L.EQ.3) .AND. PAR(2).EQ.0.) PAR(2)=PAR(1)
      IF(L.EQ.3 .AND. PAR(3).EQ.0.) PAR(3)=PAR(2)
      GOTO5019
C
 1400 RETURN
      END
C
C
C
      SUBROUTINE GEOMINC
C
      DIMENSION X(25)
      COMMON/MINCDAT/J,NVOL,WHERE,VOL(25),A(25),D(25)
      COMMON/PROXI/L,TYPE(10),PAR(7)
      COMMON/CON/ABC(26)
      DATA DELTA/1.E-8/
C
      IF(NVOL.GE.J) GOTO3
C
C-----COME HERE TO ASSIGN EQUAL VOLUMINA TO SUBDIVISIONS WHICH HAVE NOT
C     BEEN EXPLICITLY SPECIFIED-----
C
      VEX=0.
      DO4 M=1,NVOL
      IF(WHERE.EQ.4HOUT ) VEX=VEX+VOL(M)
    4 IF(WHERE.EQ.4HIN  ) VEX=VEX+VOL(J+1-M)
C     VEX IS THE TOTAL EXPLICITLY ASSIGNED VOLUME FRACTION.
C
      IF(VEX.GE.1.) GOTO10
C
      VF=(1.-VEX)/FLOAT(J-NVOL)
C-----VF IS THE VOLUME FRACTION FOR PARTITIONS WHICH ARE NOT
C     EXPLICITLY ASSIGNED.
      NVOL1=NVOL+1
      DO5 M=NVOL1,J
      IF(WHERE.EQ.4HOUT ) VOL(M)=VF
    5 IF(WHERE.EQ.4HIN  ) VOL(J+1-M)=VF
      GOTO3
C
   10 CONTINUE
C-----COME HERE IF EXPLICITLY ASSIGNED VOLUMINA EXCEED 100%-----
      PRINT 11,VEX
   11 FORMAT(# PROGRAM STOPS BECAUSE TOTAL VOLUME VEX = #E12.6,
     X# > 100%  ---  NEED TO CORRECT INPUT DATA#)
      STOP
C
    3 CONTINUE
C
C-----NOW FIND DISTANCES FROM FRACTURES WHICH CORRESPOND TO
C     DESIRED VOLUME FRACTIONS.
C     INDEXING STARTS AT THE OUTSIDE; I.E. *1* IS THE OUTERMOST
C     VOLUME ELEMENT, AND *J* IS THE INNERMOST ONE.
```

```
C-----INITIALIZE TOTAL VOLUME FRACTION.
      TVOL=0.

C-----FIRST INTERFACE WILL BE AT FRACTURE FACE.
      X(1)=0.
      D(1)=0.
      A(1)=(1.-VOL(1))*PROX(1.E-10)/1.E-10

C
C-----INITIALIZE SEARCH INTERVAL.
C
      XL=0.
      XR=VOL(2)/A(1)

C
C
      DO 30 M=2,J
C
C-----COMPUTE TOTAL FRACTION OF MATRIX VOLUME.
      TVOL=TVOL+VOL(M)/(1.-VOL(1))
      IF(M.EQ.J) TVOL=1.-1.E-9
C
      CALL INVER(TVOL,XMID,XL,XR)
C
      X(M)=XMID
C
      XMD=XMID*DELTA
      A(M)=(1.-VOL(1))*(PROX(XMID+XMD)-PROX(XMID-XMD))/(2.*XMD)
C
      D(M)=(X(M)-X(M-1))/2.
C
C-----PUT LEFT END OF NEXT ITERATION INTERVAL AT PRESENT X.
      XL=XMID
C
   30 CONTINUE
C
C
C-----COME HERE TO COMPUTE A QUASI-STEADY VALUE FOR INNERMOST
C     NODAL DISTANCE.
C
      GOTO (41,42,43,44,45,46,47,48,49,50),L
C
   41 CONTINUE
C----- ONE-D CASE.
      D(J)=(PAR(1)-2.*X(J-1))/6.
      GOTO 40
C
   42 CONTINUE
C----- TWO-D CASE.
      U=PAR(1)-2.*X(J-1)
      V=PAR(2)-2.*X(J-1)
      D(J)=U*V/(4.*(U+V))
      GOTO 40
C
```

```
   43 CONTINUE
C----- THRED CASE.
       U=PAR(1)-2*X(J-1)
       V=PAR(2)-2*X(J-1)
       W=PAR(3)-2*X(J-1)
       D(J)=3.*U*V*W/(10.*(U*V+V*W+U*W))
       GOTO 40
C
   44 CONTINUE
   45 CONTINUE
   46 CONTINUE
   47 CONTINUE
   48 CONTINUE
   49 CONTINUE
   50 CONTINUE
      D(J)=(X(J)-X(J-1))/5.
C
   40 CONTINUE
C
C-----PRINT OUT GEOMETRY DATA.
       PRINT 27
   27 FORMAT(1H1,/# ==================== GEOMETRY DATA, NORMALIZED
     XDOMAIN OF UNIT VOLUME ========================#//)
C
       PRINT 23
   23 FORMAT(#  CONTINUUM      IDENTIFIER        VOLUME       NODAL DI
     XE       INTERFACE AREA   INTERFACE DISTANCE#)
       PRINT 24
   24 FORMAT(84X,#FROM FRACTURES#/)
       PRINT 25,VOL(1),D(1)
   25 FORMAT(26H  1-FRACTURES       *1*     ,2(4XE12.6))
       PRINT 26,A(1),X(1)
   26 FORMAT(66XE12.6,7XE12.6)
C
       DO 100 M=2,J
       PRINT 101,M,ABC(M-1),VOL(M),D(M)
  101 FORMAT(* *I2,1H-*MATRIX*9X1H*,A1,1H*,8XE12.6,4XE12.6)
       IF(M.NE.J) PRINT 102,A(M),X(M)
  102 FORMAT(66XE12.6,7XE12.6)
  100 CONTINUE
C
       PRINT 103
  103 FORMAT(/100(1H=))
C
       RETURN
       END
C
C
C
       FUNCTION PROX(X)
C
C-----THE PROXIMITY FUNCTION PROX(X) REPRESENTS THE FRACTION OF
C     MATRIX VOLUME [VM=(1.-VOL(1))*VO WITHIN A DOMAIN VO] WHICH
C     IS WITHIN A DISTANCE X FROM THE FRACTURES.
```

```
      COMMON/PROXI/L,TYPE(10),PAR(7)
      NOW ASSIGN DATA FOR STANFORD LARGE RESERVOIR MODEL.
      DATA A,B,C,D/.263398,.190754,.2032,.191262/

      GOTO(1,2,3,4,4,4,1,1,1,1),L

    1 CONTINUE
C---- ONE-D CASE.
      PROX=2.*X/PAR(1)
      IF(X.GE.PAR(1)/2.) PROX=1.
      RETURN
C
    2 CONTINUE
C---- TWO-D CASE.
C     THE MATRIX BLOCKS HAVE THICKNESS OF PAR(1) AND PAR(2),
C     RESPECTIVELY, MEASURED PERPENDICULAR TO THE FRACTURES.
C     THE PROXIMITY FUNCTION IS VALID FOR ARBITRARY ANGLE
C     BETWEEN THE FRACTURE SETS.
      PROX=2.*(PAR(1)+PAR(2))*X/(PAR(1)*PAR(2))
     X-4.*X*X/(PAR(1)*PAR(2))
      IF(X.GE.PAR(1)/2. .OR. X.GE.PAR(2)/2.) PROX=1.
      RETURN
C
    3 CONTINUE
C---- THREE DIMENSIONAL CASE.
      U=2.*X/PAR(1)
      V=2.*X/PAR(2)
      W=2.*X/PAR(3)
      PROX=U*V*W-(U*V+U*W+V*W)+U+V+W
      IF(U.GE.1. .OR. V.GE.1. .OR. W.GE.1.) PROX=1.
      RETURN
C
    4 CONTINUE
C***** MATRIX OF STANFORD LARGE RESERVOIR MODEL *****
C
C
C     RECTANGULAR BLOCKS IN LAYERS B1,B2,M1,M2,T1.
      VR=8.*X**3-(8.*B+4.*A)*X**2+(4.*A*B+2.*B**2)*X
      IF(X.GE.B/2.) VR=A*B*B
C
C     TRIANGULAR BLOCKS IN LAYERS B1,B2,M1,M2,T1.
      VT=(6.+4.*SQRT(2.))*X**3
     X-(A*(6.+4.*SQRT(2.))/2.+2.*B*(2.+SQRT(2.)))*X**2
     X+(A*B*(2.+SQRT(2.))+B*B)*X
      IF(X.GE.B/(2.+SQRT(2.))) VT=A*B*B/2.
C
C     RECTANGULAR BLOCKS IN LAYER T2.
      VRT2=8.*X**3-(8.*D+4.*C)*X**2+(4.*C*D+2.*D**2)*X
      IF(X.GE.D/2.) VRT2=C*D*D
C
C     TRIANGULAR BLOCKS IN LAYER T2.
      VTT2=(6.+4.*SQRT(2.))*X**3
     X-(C*(6.+4.*SQRT(2.))/2.+2.*D*(2.+SQRT(2.)))*X**2
```

```
      X+(C*D*(2.+SQRT(2.))+D*D)*X
       IF(X.GE.D/(2.+SQRT(2.)))  VTT2=C*D*D/2.
C
       IF(L.EQ.4)  GOTO 14
       IF(L.EQ.5)  GOTO 15
       IF(L.EQ.6)  GOTO 16
C
C***** NOW COMPUTE TOTAL MATRIX VOLUME WITHIN DISTANCE X.
   14  V=5.*(5.*VR+4.*VT)+5.*VRT2+4.*VTT2
C-----AVERAGE PROXIMITY FUNCTION FOR ENTIRE ROCK LOADING.
C
       VTOT=35.*A*B**2+7.*C*D**2
C      VOLUME FRACTION.
       PROX=V/VTOT
       RETURN
C
   15  PROX=(5.*VR+4.*VT)/(7.*A*B*B)
C-----PROXIMITY FUNCTION FOR FIVE BOTTOM LAYERS.
       RETURN
C
   16  PROX=(5.*VRT2+4.*VTT2)/(7.*C*D*D)
C-----PROXIMITY FUNCTION FOR TOP LAYER.
       RETURN
C
C
       END
C
C
C
       SUBROUTINE INVER(F,X,XL,XR)
C
C===== THIS ROUTINE INVERTS THE PROXIMITY FUNCTION, TO GIVE A
C      DISTANCE *X* FROM FRACTURE FACES FOR A DESIRED FRACTION *F* OF
C      MATRIX VOLUME.
C
       DATA TOL/1.E-10/
C
C-----CHECK AND ADJUST UPPER LIMIT OF SEARCH INTERVAL.
   22  FR=PROX(XR)
       IF(FR.GT.F)  GOTO 20
       XR=2.*XR
       GOTO 22
C
C-----PERFORM ITERATIVE BISECTING, TO OBTAIN A SEQUENCE OF NESTED
C      INTERVALS CONTAINING THE DESIRED POINT, X.
   20  XMID=(XR+XL)/2.
       IF(XR-XL.LE.TOL*XR)  GOTO 21
       FMID=PROX(XMID)
       IF(FMID.LE.F)  XL=XMID
       IF(FMID.GE.F)  XR=XMID
       GOTO 20
C
   21  CONTINUE
C-----COME HERE FOR CONVERGENCE.
```

```
      X=XMID
      RETURN
      END



      SUBROUTINE MINCME
C===== THIS ROUTINE WORKS SEQUENTIALLY THROUGH THE ELEMENTS OF THE
C     PRIMARY MESH, ASSIGNING ALL SECONDARY ELEMENTS AND INTRA-BLOCK
C     CONNECTIONS.
C
C
      COMMON/MINCDAT/J,NVOL,WHERE,VOL(25),A(25),D(25)
      COMMON/PROXI/L,TYPE(10),PAR(7)
      COMMON/CON/ABC(26)
      DIMENSION DENT(16)
C
      REWIND 4
      READ(4,1) (DENT(I),I=1,16)
    1 FORMAT(16A5)
      WRITE(14,2) (DENT(I),I=1,12),J,NVOL,WHERE,TYPE(L)
    2 FORMAT(12A5,5H *** ,2I3,A4,A5)
    9 READ(4,10) EL1,EL2,NE,MA0,MA1,MA2,VOLX
   10 FORMAT(A2,A1,I2,10XA1,A2,A2,E10.4)
      IF(EL1.EQ.2H  .AND.EL2.EQ.1H .AND.NE.EQ.0) GOTO40
C
C-----FOR EACH PRIMARY ELEMENT, ASSIGN *J* SECONDARY ELEMENTS.
      DO11 M=1,J
      V=VOL(M)*VOLX
      IF(M.EQ.1) WRITE(14,14) EL1,M,NE,MA0,MA1,MA2,V
      IF(M.NE.1) WRITE(14,15) EL1,ABC(M-1),NE,MA1,MA2,V
   14 FORMAT(A2,I1,I2,10XA1,A2,A2,E10.4)
   15 FORMAT(A2,A1,I2,10X1HM,A2,A2,E10.4)
C
      IF(M.EQ.1) GOTO100
C-----COME HERE TO WRITE INTRA-BLOCK CONNECTIONS-----
C
      AREA=VOLX*A(M-1)
      M1=M-1
      IF(M.EQ.2) WRITE(15,104) EL10,M1,NE0,EL1,ABC(M-1),MA2,D(M-1),
     XD(M),AREA
  104 FORMAT(A2,I1,I2,A2,A1,I2,19X1H1,3E10.4)
      IF(M.NE.2)
     XWRITE(15,102) EL10,ABC(M1-1),NE0,EL1,ABC(M-1),MA2,D(M-1),D(M),AREA
  102 FORMAT(2(A2,A1,I2),19X1H1,3E10.4)
C
  100 EL10=EL1
C     EL20=EL2
      NE0=NE
C
   11 CONTINUE
C
      GOTO9
C
```

```
   40 WRITE(14,103)
      WRITE(15,103)
  103 FORMAT(#      #)
C
      RETURN
      END
```

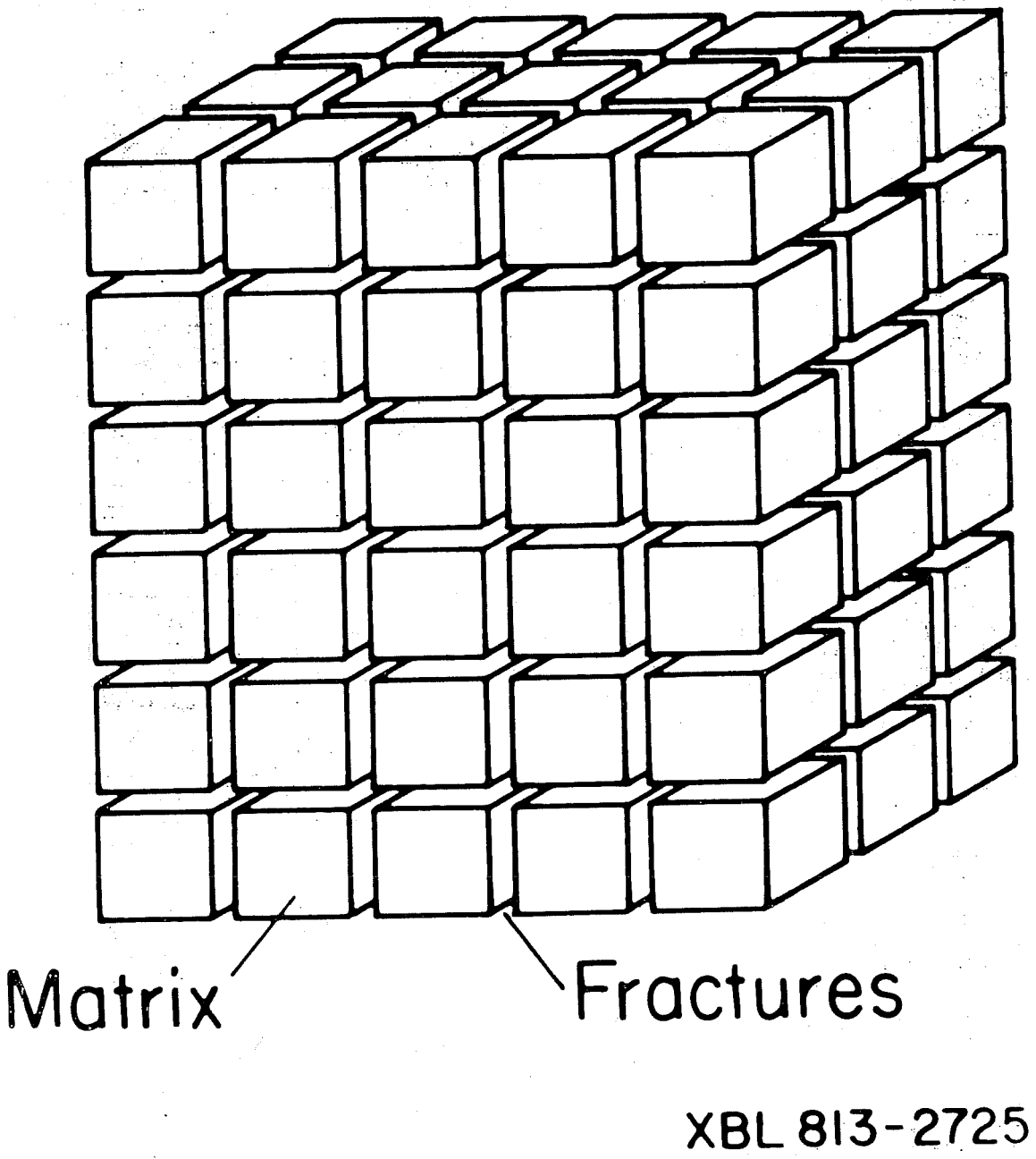

Figure 1. Idealized model of a fractured porous medium.

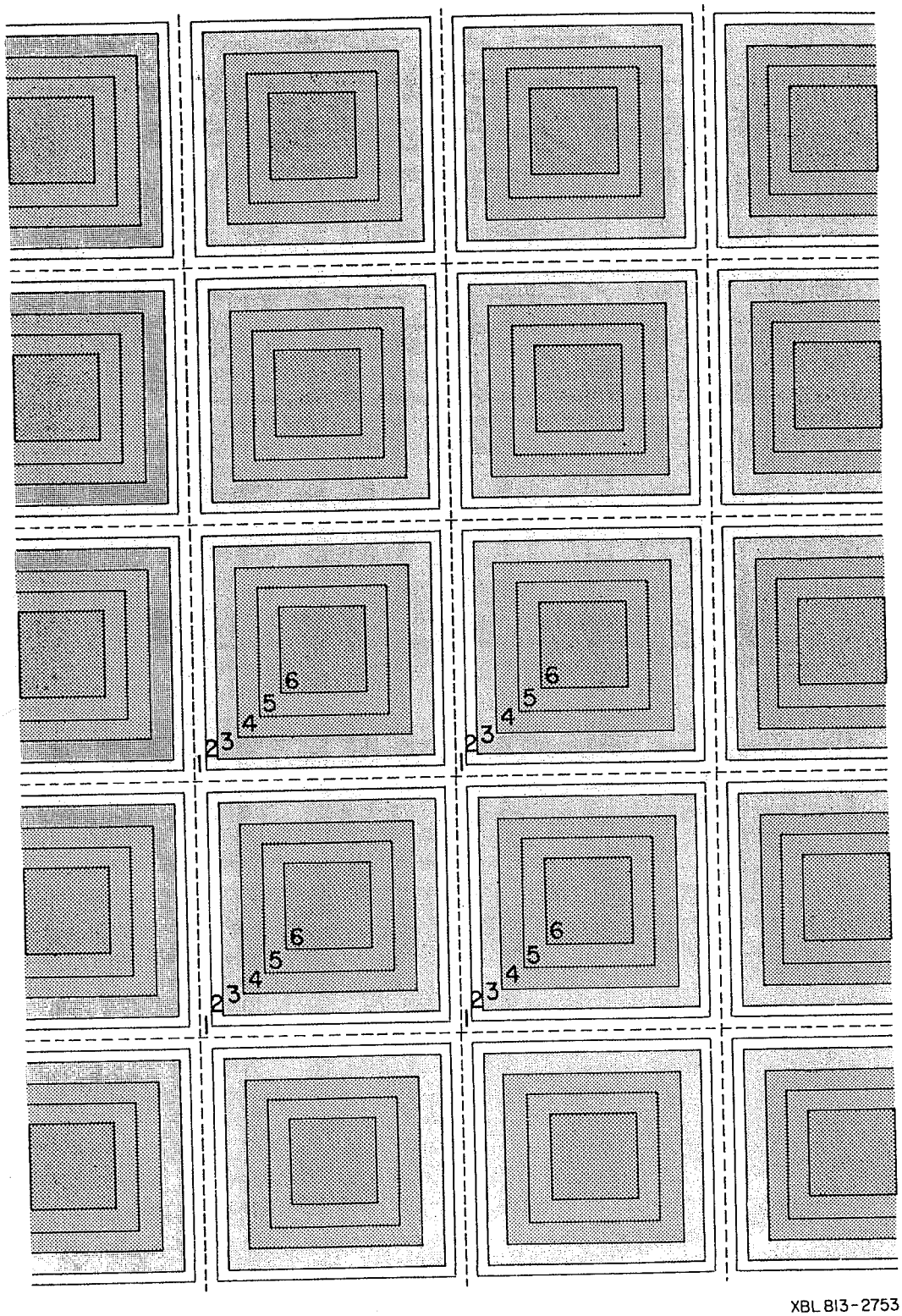

Figure 2. Basic computational mesh for a fractured porous medium.

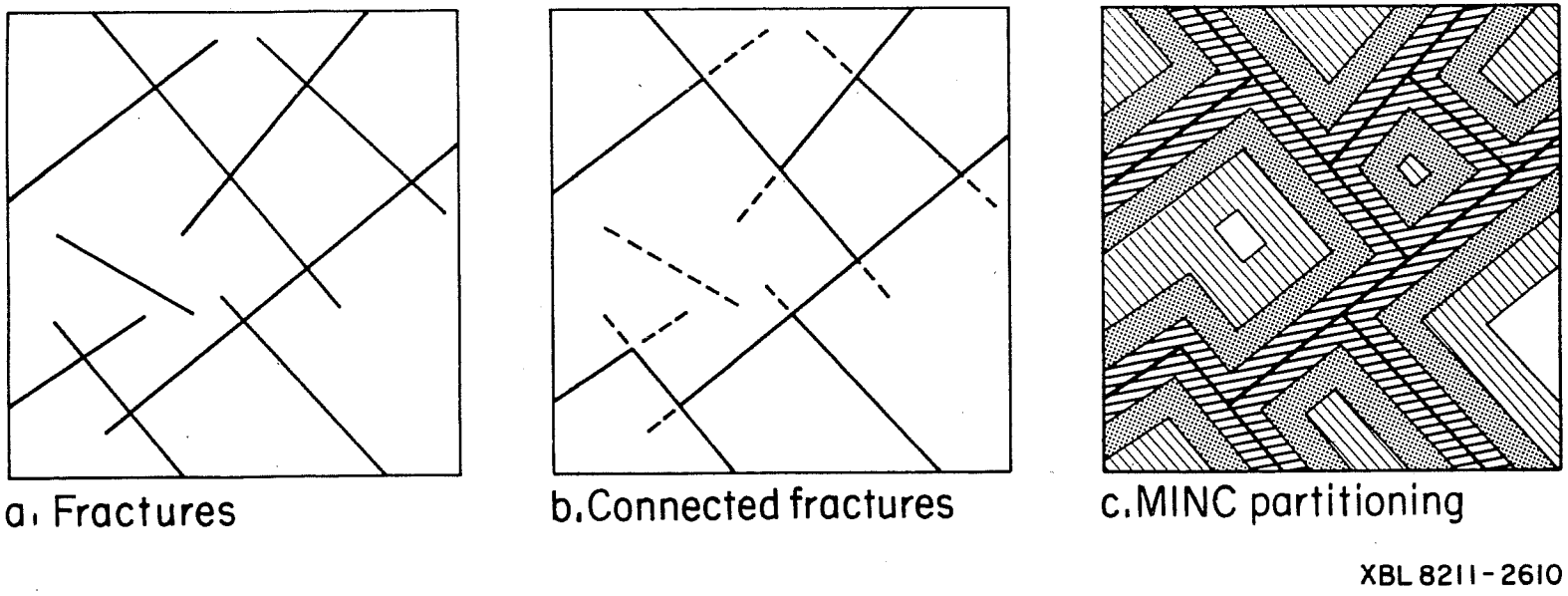

Figure 3. MINC-concept for an arbitrary two-dimensional fracture distribution.

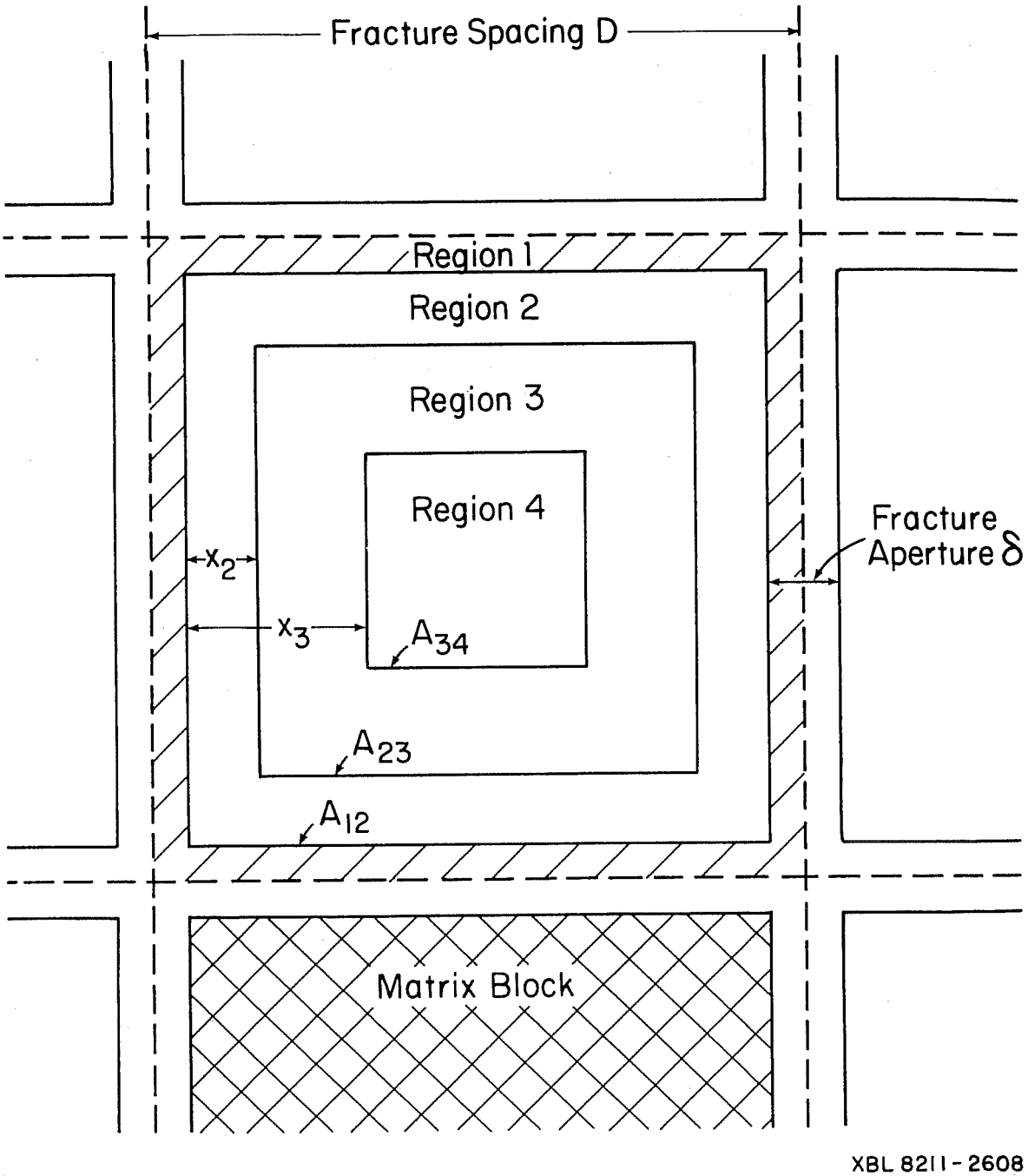

Figure 4. MINC-partitioning for an idealized fracture system.

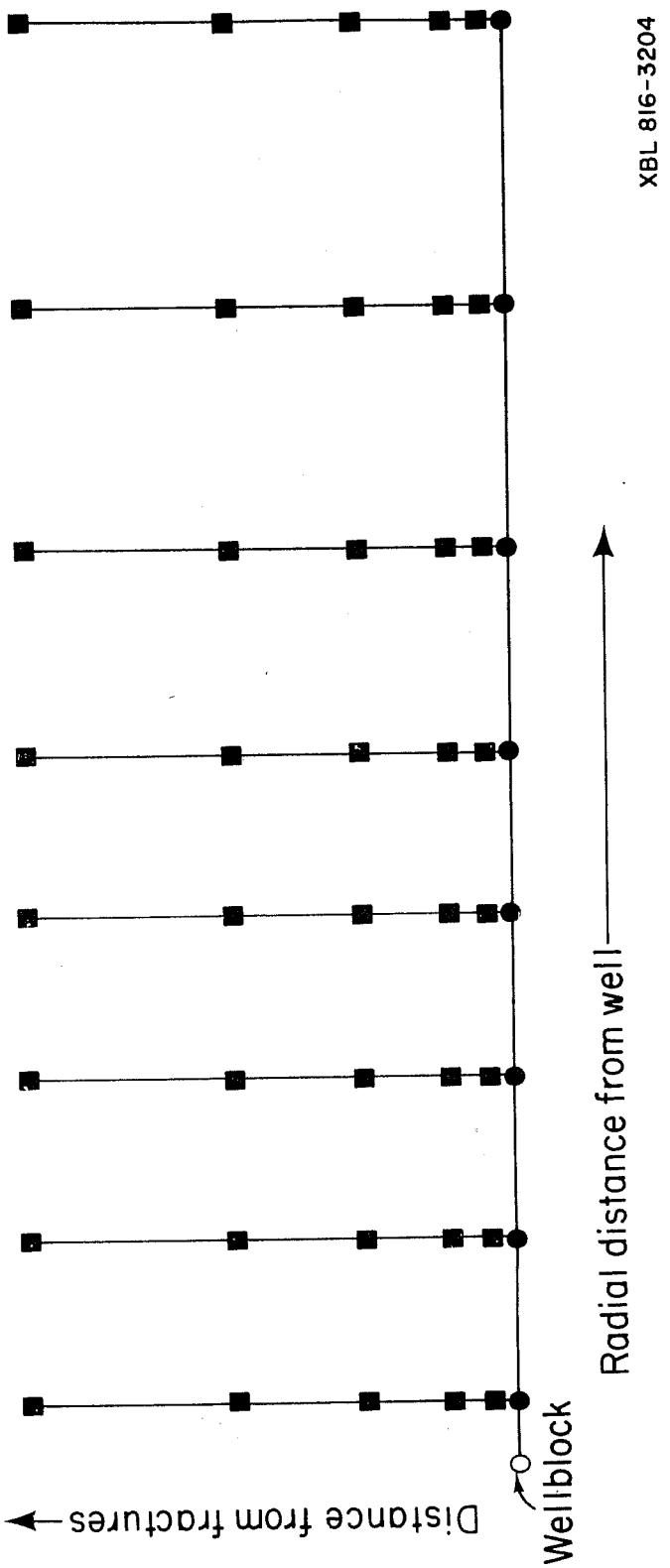

Figure 5. Schematic diagram of a MINC-mesh for a radial flow problem.

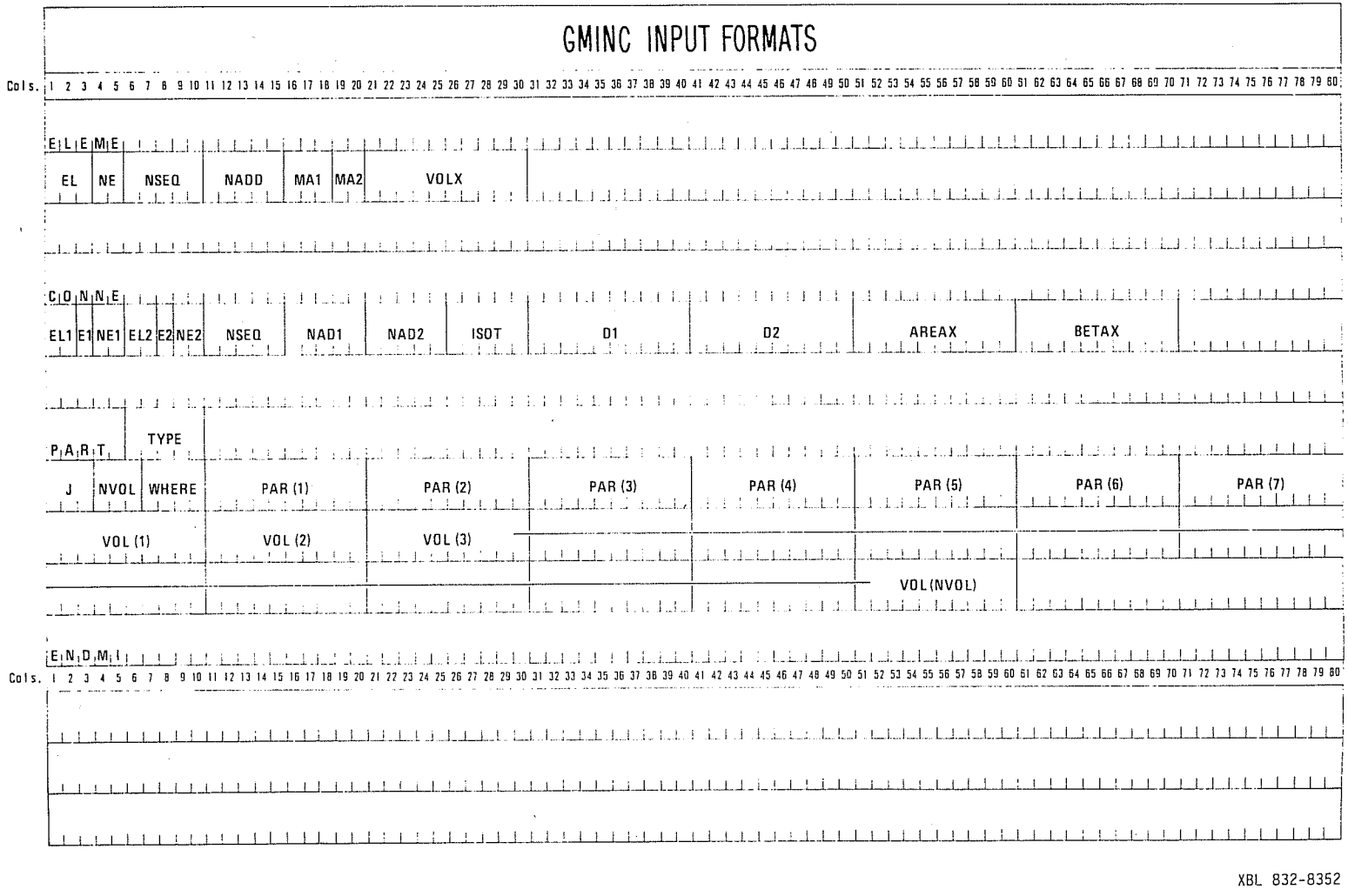

Figure 6. GMINC input formats.

```
GMIN,07,63.466601,PRUESS
*INPUT 6600B 10.55.42  10 FEB 83  VIA KP00000
*HOLDOUT
.....DIABLO,RGMINC.....
LIBCOPY,DIABLO,LGO,GMINCG.
REWIND,LGO.
LINK,X.
COPY,TAPE14/RB,ORXR,TAPE15/RB,ORXR,MESH.
COPYSBF,MESH,OUTPUT.
EXIT.
DUMP,0.
FIN.
REWIND,INPUT.
COPYSBF,INPUT,OUTPUT.


ELEME
F   1          ROCK 100.

CONNE

PART THRED
 10  90UT 50.
    .01E-2    .09E-2     .9E-2     2.E-2     4.E-2    10.E-2    20.E-2    30.E-2
    20.E-2
ENDMI
```

Figure 7. GMINC input deck for one-block problem

========== GEOMETRY DATA, NORMALIZED TO A DOMAIN OF UNIT VOLUME ==========

CONTINUUM	IDENTIFIER	VOLUME	NODAL DISTANCE	INTERFACE AREA	INTERFACE DISTANCE FROM FRACTURES
1-FRACTURES	*1*	.100000E-03	0.		
				.119988E+00	0.
2-MATRIX	*A*	.900000E-03	.375150E-02		
				.119916E+00	.750300E-02
3-MATRIX	*B*	.900000E-02	.376395E-01		
				.119195E+00	.827821E-01
4-MATRIX	*C*	.200000E-01	.844677E-01		
				.117584E+00	.251718E+00
5-MATRIX	*D*	.400000E-01	.172484E+00		
				.114329E+00	.596686E+00
6-MATRIX	*E*	.100000E+00	.454020E+00		
				.105979E+00	.150473E+01
7-MATRIX	*F*	.200000E+00	.103151E+01		
				.881848E-01	.356774E+01
8-MATRIX	*G*	.300000E+00	.207781E+01		
				.573028E-01	.772337E+01
9-MATRIX	*H*	.200000E+00	.230586E+01		
				.307937E-01	.123351E+02
10-MATRIX	*I*	.130000E+00	.253298E+01		

==========

Figure 8. Geometry data for MINC-partitioning of one-block problem.

```
ELEME                                                          ***  10  9OUT THRED
F 1 1           ROCK   .1000E-01
F A 1           MOCK   .9000E-01
F B 1           MOCK   .9000E+00
F C 1           MOCK   .2000E+01
F D 1           MOCK   .4000E+01
F E 1           MOCK   .1000E+02
F F 1           MOCK   .2000E+02
F G 1           MOCK   .3000E+02
F H 1           MOCK   .2000E+02
F I 1           MOCK   .1300E+02

CONNE
F 1 1F A 1                    10.          .3752E-02 .1200E+02
F A 1F B 1                    1 .3752E-02 .3764E-01 .1199E+02
F B 1F C 1                    1 .3764E-01 .8447E-01 .1192E+02
F C 1F D 1                    1 .8447E-01 .1725E+00 .1176E+02
F D 1F E 1                    1 .1725E+00 .4540E+00 .1143E+02
F E 1F F 1                    1 .4540E+00 .1032E+01 .1060E+02
F F 1F G 1                    1 .1032E+01 .2078E+01 .8818E+01
F G 1F H 1                    1 .2078E+01 .2306E+01 .5730E+01
F H 1F I 1                    1 .2306E+01 .2533E+01 .3079E+01
```

Figure 9. Secondary mesh for one-block problem

```
BBBB,07,63.466601,PRUESS
*INPUT 6600B 10.59.48  10 FEB 83  VIA KP00000
*HOLDOUT
.....DIABLO,BBBB.....
LIBCOPY,DIABLO,LGO,GMINCG.
REWIND,LGO.
LINK,X.
COPY,TAPE14/RB,ORXR,TAPE15/RB,ORXR,MESH.
COPYSBF,MESH,OUTPUT.
EXIT.
DUMP,0.
FIN.
REWIND,INPUT.
COPYSBF,INPUT,OUTPUT.


ELEME
COL 1     4     1GRAYW        1.E8

CONNE
COL 1COL 2     3     1     1     3 50.        50.                  1.E6 1.

PART TWO-D
  6  4OUT 20.          40.
     1.E-2       4.E-2       10.E-2      25.E-2
ENDMI
```

Figure 10. GMINC input deck for vertical column

========== GEOMETRY DATA, NORMALIZED TO A DOMAIN OF UNIT VOLUME ==========

CONTINUUM	IDENTIFIER	VOLUME	NODAL DISTANCE	INTERFACE AREA	INTERFACE DISTANCE FROM FRACTURES
1-FRACTURES	*1*	.100000E-01	0.		
				.148500E+00	0.
2-MATRIX	*A*	.400000E-01	.135912E+00		
				.145809E+00	.271823E+00
3-MATRIX	*B*	.100000E+00	.351293E+00		
				.138853E+00	.974410E+00
4-MATRIX	*C*	.250000E+00	.966885E+00		
				.119709E+00	.290818E+01
5-MATRIX	*D*	.300000E+00	.141973E+01		
				.915983E-01	.574765E+01
6-MATRIX	*E*	.300000E+00	.163758E+01		

Figure 11. Geometry data for MINC-partitioning of vertical column.

```
                                                                    ***    6  4001
ELEME
C01 1          GRAYW  .1000E+07
COA 1          MRAYW  .4000E+07
COB 1          MRAYW  .1000E+08
COC 1          MRAYW  .2500E+08
COD 1          MRAYW  .3000E+08
COE 1          MRAYW  .3000E+08
C01 2          GRAYW  .1000E+07
COA 2          MRAYW  .4000E+07
COB 2          MRAYW  .1000E+08
COC 2          MRAYW  .2500E+08
COD 2          MRAYW  .3000E+08
COE 2          MRAYW  .3000E+08
C01 3          GRAYW  .1000E+07
COA 3          MRAYW  .4000E+07
COB 3          MRAYW  .1000E+08
COC 3          MRAYW  .2500E+08
COD 3          MRAYW  .3000E+08
COE 3          MRAYW  .3000E+08
C01 4          GRAYW  .1000E+07
COA 4          MRAYW  .4000E+07
COB 4          MRAYW  .1000E+08
COC 4          MRAYW  .2500E+08
COD 4          MRAYW  .3000E+08
COE 4          MRAYW  .3000E+08
C01 5          GRAYW  .1000E+07
COA 5          MRAYW  .4000E+07
COB 5          MRAYW  .1000E+08
COC 5          MRAYW  .2500E+08
COD 5          MRAYW  .3000E+08
COE 5          MRAYW  .3000E+08

CONNE
C01 1C01 2                3 -.5000E+02 -.5000E+02 -.1000E+07 -.1000E+01
C01 2C01 3                3 -.5000E+02 -.5000E+02 -.1000E+07 -.1000E+01
C01 3C01 4                3 -.5000E+02 -.5000E+02 -.1000E+07 -.1000E+01
C01 4C01 5                3 -.5000E+02 -.5000E+02 -.1000E+07 -.1000E+01
C01 1COA 1               10.           -.1359E+00 -.1485E+08
COA 1COB 1                1 -.1359E+00 -.3513E+00 -.1458E+08
COB 1COC 1                1 -.3513E+00 -.9669E+00 -.1389E+08
COC 1COD 1                1 -.9669E+00 -.1420E+01 -.1197E+08
COD 1COE 1                1 -.1420E+01 -.1638E+01 -.9160E+07
C01 2COA 2               10.           -.1359E+00 -.1485E+08
COA 2COB 2                1 -.1359E+00 -.3513E+00 -.1458E+08
COB 2COC 2                1 -.3513E+00 -.9669E+00 -.1389E+08
COC 2COD 2                1 -.9669E+00 -.1420E+01 -.1197E+08
COD 2COE 2                1 -.1420E+01 -.1638E+01 -.9160E+07
C01 3COA 3               10.           -.1359E+00 -.1485E+08
COA 3COB 3                1 -.1359E+00 -.3513E+00 -.1458E+08
COB 3COC 3                1 -.3513E+00 -.9669E+00 -.1389E+08
COC 3COD 3                1 -.9669E+00 -.1420E+01 -.1197E+08
COD 3COE 3                1 -.1420E+01 -.1638E+01 -.9160E+07
C01 4COA 4               10.           -.1359E+00 -.1485E+08
COA 4COB 4                1 -.1359E+00 -.3513E+00 -.1458E+08
COB 4COC 4                1 -.3513E+00 -.9669E+00 -.1389E+08
COC 4COD 4                1 -.9669E+00 -.1420E+01 -.1197E+08
COD 4COE 4                1 -.1420E+01 -.1638E+01 -.9160E+07
C01 5COA 5               10.           -.1359E+00 -.1485E+08
COA 5COB 5                1 -.1359E+00 -.3513E+00 -.1458E+08
COB 5COC 5                1 -.3513E+00 -.9669E+00 -.1389E+08
COC 5COD 5                1 -.9669E+00 -.1420E+01 -.1197E+08
COD 5COE 5                1 -.1420E+01 -.1638E+01 -.9160E+07
```

Figure 12. Secondary mesh for vertical column.

```
CCCC,07,63.466601,PRUESS
*INPUT 6600B 11.01.27  10 FEB 83  VIA KP00000
*HOLDOUT
.....DIABLO,CCCC.....
LIBCOPY,DIABLO,LGO,GMINCG.
REWIND,LGO.
LINK,X.
COPY,TAPE14/RB,ORXR,TAPE15/RB,ORXR,MESH.
COPYSBF,MESH,OUTPUT.
EXIT.
DUMP,0.
FIN.
REWIND,INPUT.
COPYSBF,INPUT,OUTPUT.
```

```
ELEME
AA  1                1 .3142E+03
AA  2                1 .2969E+04
AA  3                1 .1793E+05
AA  4                1 .9636E+05
AA  5                1 .4959E+06
AA  6                1 .2507E+07
AA  7                1 .1257E+08
AA  8                1 .6285E+08

CONNE
AA  1AA  2                    1 .5000E+00 .1116E+01 .6283E+03
AA  2AA  3                    1 .1116E+01 .2492E+01 .2031E+04
AA  3AA  4                    1 .2492E+01 .5564E+01 .5163E+04
AA  4AA  5                    1 .5564E+01 .1242E+02 .1216E+05
AA  5AA  6                    1 .1242E+02 .2774E+02 .2777E+05
AA  6AA  7                    1 .2774E+02 .6192E+02 .6262E+05
AA  7AA  8                    1 .6192E+02 .1382E+03 .1404E+06

PART ONE-D
  5  2OUT 10.
     2.E-2      8.E-2
ENDMI
```

Figure 13. GMINC input deck for radial flow system.

========== GEOMETRY DATA, NORMALIZED TO A DOMAIN OF UNIT VOLUME ==========

CONTINUUM	IDENTIFIER	VOLUME	NODAL DISTANCE	INTERFACE AREA	INTERFACE DISTANCE FROM FRACTURES
1-FRACTURES	*1*	.200000E-01	0.	.196000E+00	0.
2-MATRIX	*A*	.800000E-01	.204082E+00	.196000E+00	.408163E+00
3-MATRIX	*B*	.300000E+00	.765306E+00	.196000E+00	.193878E+01
4-MATRIX	*C*	.300000E+00	.765306E+00	.196000E+00	.346939E+01
5-MATRIX	*D*	.300000E+00	.510204E+00		

Figure 14. Geometry data for MINC-partitioning of radial flow system.

```
ELEME                                                    ***   5  2OUT ONE-D
AA1 1                1 .6284E+01
AAA 1           M    1 .2514E+02
AAB 1           M    1 .9426E+02
AAC 1           M    1 .9426E+02
AAD 1           M    1 .9426E+02
AA1 2                1 .5938E+02
AAA 2           M    1 .2375E+03
AAB 2           M    1 .8907E+03
AAC 2           M    1 .8907E+03
AAD 2           M    1 .8907E+03
AA1 3                1 .3586E+03
AAA 3           M    1 .1434E+04
AAB 3           M    1 .5379E+04
AAC 3           M    1 .5379E+04
AAD 3           M    1 .5379E+04
AA1 4                1 .1927E+04
AAA 4           M    1 .7709E+04
AAB 4           M    1 .2891E+05
AAC 4           M    1 .2891E+05
AAD 4           M    1 .2891E+05
AA1 5                1 .9918E+04
AAA 5           M    1 .3967E+05
AAB 5           M    1 .1488E+06
AAC 5           M    1 .1488E+06
AAD 5           M    1 .1488E+06
AA1 6                1 .5014E+05
AAA 6           M    1 .2006E+06
AAB 6           M    1 .7521E+06
AAC 6           M    1 .7521E+06
AAD 6           M    1 .7521E+06
AA1 7                1 .2514E+06
AAA 7           M    1 .1006E+07
AAB 7           M    1 .3771E+07
AAC 7           M    1 .3771E+07
AAD 7           M    1 .3771E+07
AA1 8                1 .1257E+07
AAA 8           M    1 .5028E+07
AAB 8           M    1 .1886E+08
AAC 8           M    1 .1886E+08
AAD 8           M    1 .1886E+08

CONNE
AA1 1AA1 2                    1 .5000E+00 .1116E+01 .6283E+03-.0
AA1 2AA1 3                    1 .1116E+01 .2492E+01 .2031E+04-.0
AA1 3AA1 4                    1 .2492E+01 .5564E+01 .5163E+04-.0
AA1 4AA1 5                    1 .5564E+01 .1242E+02 .1216E+05-.0
AA1 5AA1 6                    1 .1242E+02 .2774E+02 .2777E+05-.0
AA1 6AA1 7                    1 .2774E+02 .6192E+02 .6262E+05-.0
AA1 7AA1 8                    1 .6192E+02 .1382E+03 .1404E+06-.0
AA1 1AAA 1                    10.         .2041E+00 .6158E+02
AAA 1AAB 1                    1 .2041E+00 .7653E+00 .6158E+02
AAB 1AAC 1                    1 .7653E+00 .7653E+00 .6158E+02
AAC 1AAD 1                    1 .7653E+00 .5102E+00 .6158E+02
AA1 2AAA 2                    10.         .2041E+00 .5819E+03
AAA 2AAB 2                    1 .2041E+00 .7653E+00 .5819E+03
AAB 2AAC 2                    1 .7653E+00 .7653E+00 .5819E+03
AAC 2AAD 2                    1 .7653E+00 .5102E+00 .5819E+03
AA1 3AAA 3                    10.         .2041E+00 .3514E+04
AAA 3AAB 3                    1 .2041E+00 .7653E+00 .3514E+04
AAB 3AAC 3                    1 .7653E+00 .7653E+00 .3514E+04
AAC 3AAD 3                    1 .7653E+00 .5102E+00 .3514E+04
AA1 4AAA 4                    10.         .2041E+00 .1889E+05
AAA 4AAB 4                    1 .2041E+00 .7653E+00 .1889E+05
AAB 4AAC 4                    1 .7653E+00 .7653E+00 .1889E+05
AAC 4AAD 4                    1 .7653E+00 .5102E+00 .1889E+05
AA1 5AAA 5                    10.         .2041E+00 .9720E+05
AAA 5AAB 5                    1 .2041E+00 .7653E+00 .9720E+05
AAB 5AAC 5                    1 .7653E+00 .7653E+00 .9720E+05
AAC 5AAD 5                    1 .7653E+00 .5102E+00 .9720E+05
AA1 6AAA 6                    10.         .2041E+00 .4914E+06
AAA 6AAB 6                    1 .2041E+00 .7653E+00 .4914E+06
AAB 6AAC 6                    1 .7653E+00 .7653E+00 .4914E+06
AAC 6AAD 6                    1 .7653E+00 .5102E+00 .4914E+06
AA1 7AAA 7                    10.         .2041E+00 .2464E+07
AAA 7AAB 7                    1 .2041E+00 .7653E+00 .2464E+07
AAB 7AAC 7                    1 .7653E+00 .7653E+00 .2464E+07
AAC 7AAD 7                    1 .7653E+00 .5102E+00 .2464E+07
AA1 8AAA 8                    10.         .2041E+00 .1232E+08
AAA 8AAB 8                    1 .2041E+00 .7653E+00 .1232E+08
AAB 8AAC 8                    1 .7653E+00 .7653E+00 .1232E+08
AAC 8AAD 8                    1 .7653E+00 .5102E+00 .1232E+08
```

Figure 15. Secondary mesh for radial flow system

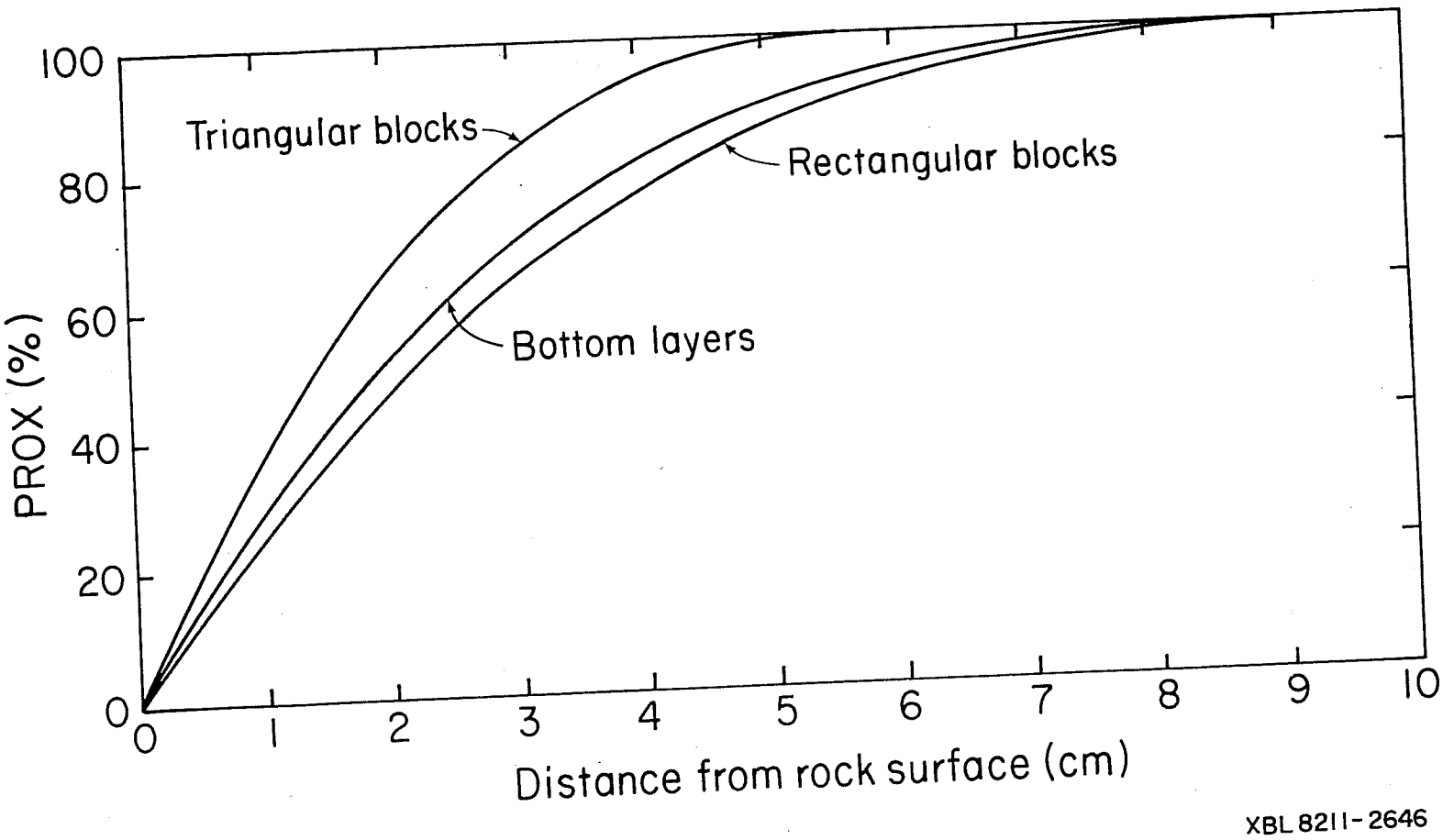

Figure 16. Proximity functions for Stanford large reservoir model.

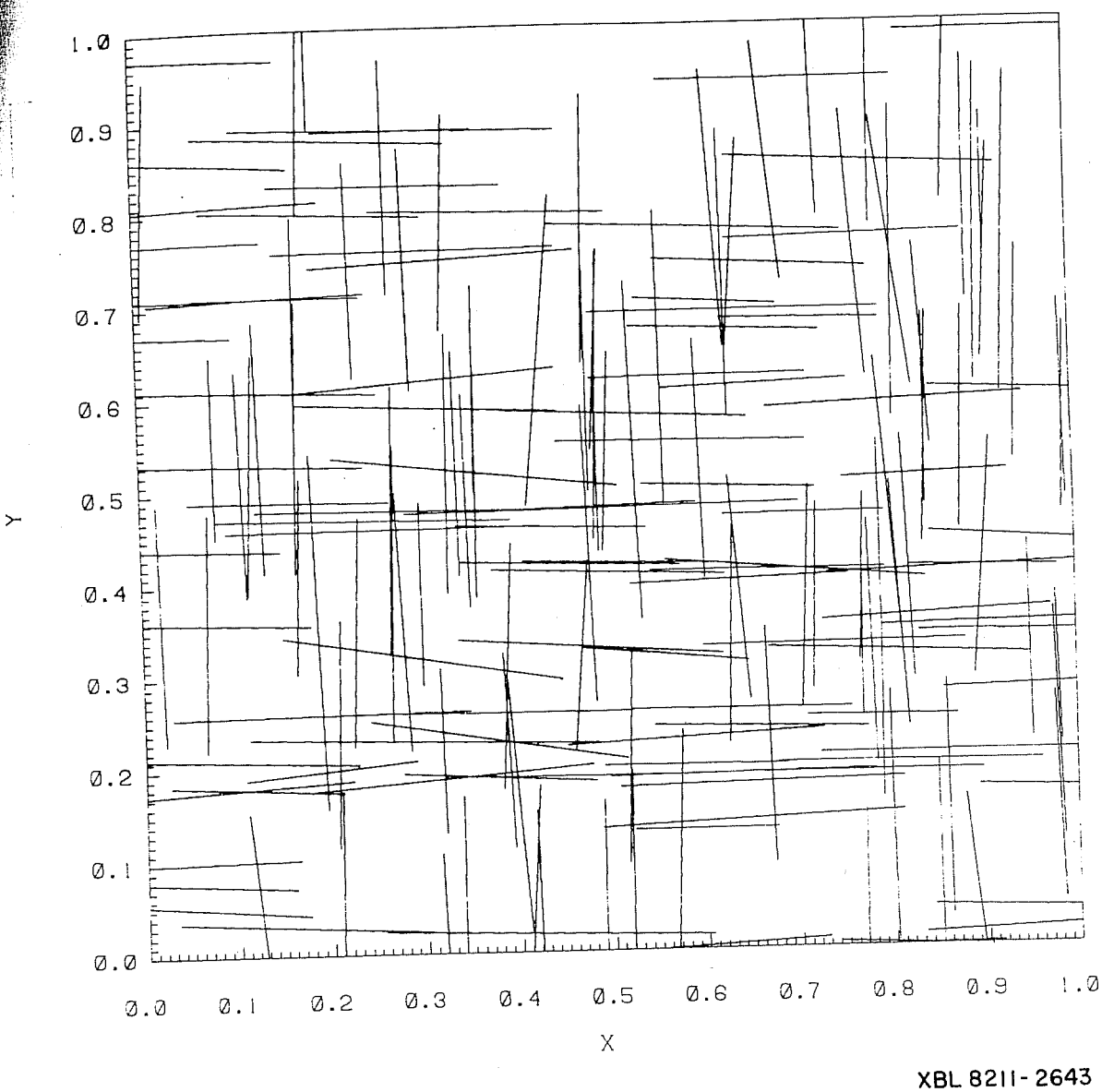

Figure 17. Two-dimensional stochastic fracture distribution.

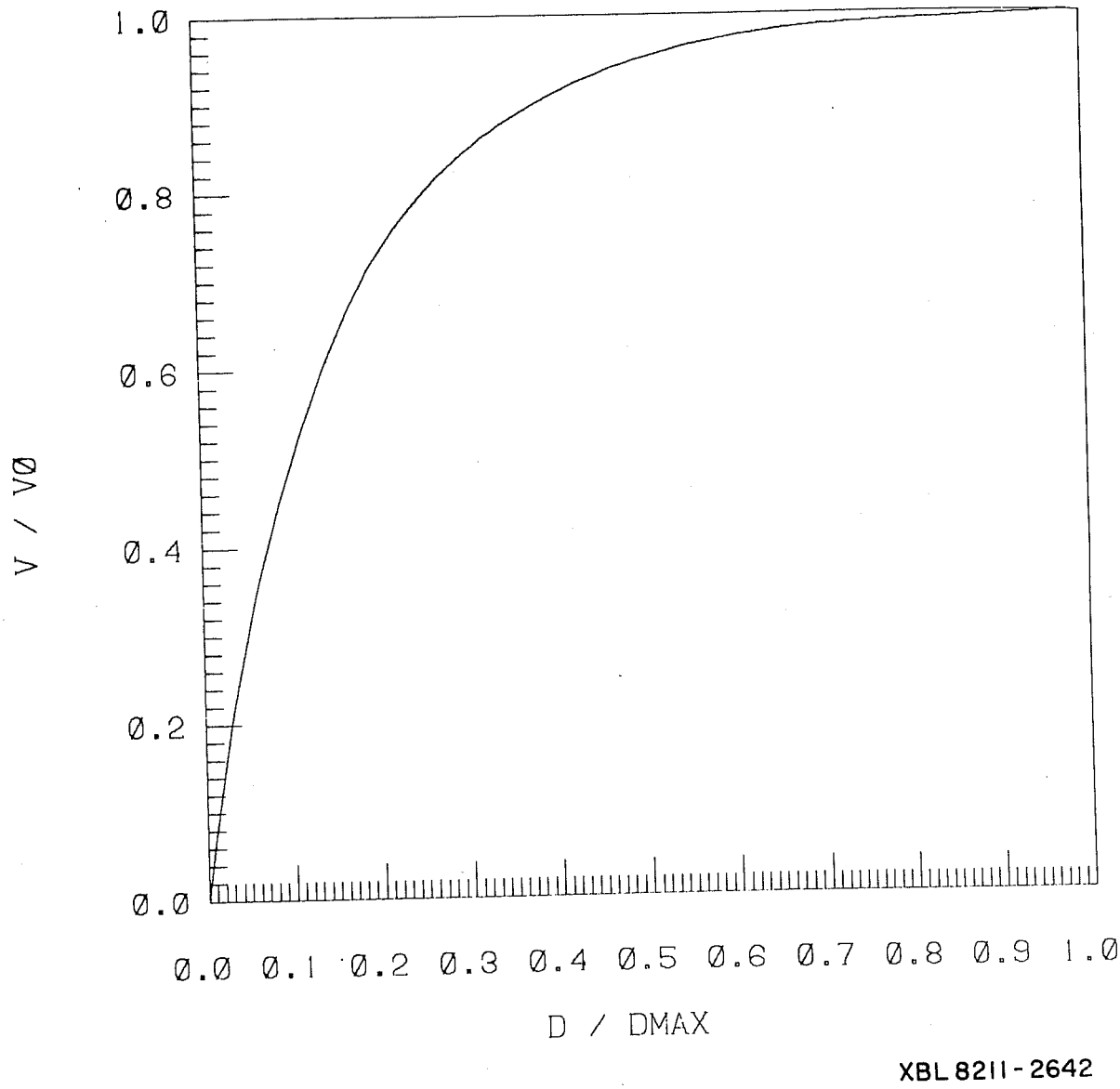

Figure 18. Proximity function for stochastic fracture distribution.

This report was done with support from the Department of Energy. Any conclusions or opinions expressed in this report represent solely those of the author(s) and not necessarily those of The Regents of the University of California, the Lawrence Berkeley Laboratory or the Department of Energy.

Reference to a company or product name does not imply approval or recommendation of the product by the University of California or the U.S. Department of Energy to the exclusion of others that may be suitable.